A

Clinical indexes	AKI (n=8)	Non-AKI (n=7)	P Value
Sex	M (4) F(4)	M (6) F (1)	0.1432
Age (year)	46.8±13.5	38.6±15.5	0.3334
Hypertension	63%	14%	0.0572
Diabetes	All negative	All negative	
BUN(mg/dL)*	45.33±19.54	15.25±5.59	0.0043
Serum Creatinine (mg/dL)*	6.14±1.81	0.85±0.15	0.0001
Diagnosis	AKI (7) ESRD/AKI (1)	FSGS (1) IgA nephropathy (3) Membranous nephropathy (2) Membranoproliferative glomerulonephritis (1)	

B

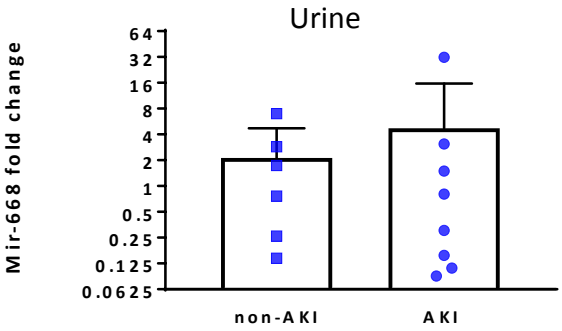

C

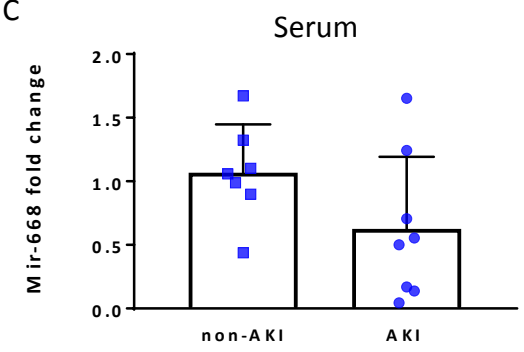

Supplementary Figure 1 (A) Clinical data of AKI and non-AKI patients examined. (Peason's Chi-Square test for Sex and hypertension frequency difference comparison and 2-tailed student's t-test for all other comparison). *, statistically significant difference between AKI and non-AKI group. (B) mir-668 in urine samples from patients (n=8 for AKI, n=6 for non-AKI). (C) mir-668 in serum samples from patients (n=8 for AKI, n=7 for non-AKI).

A

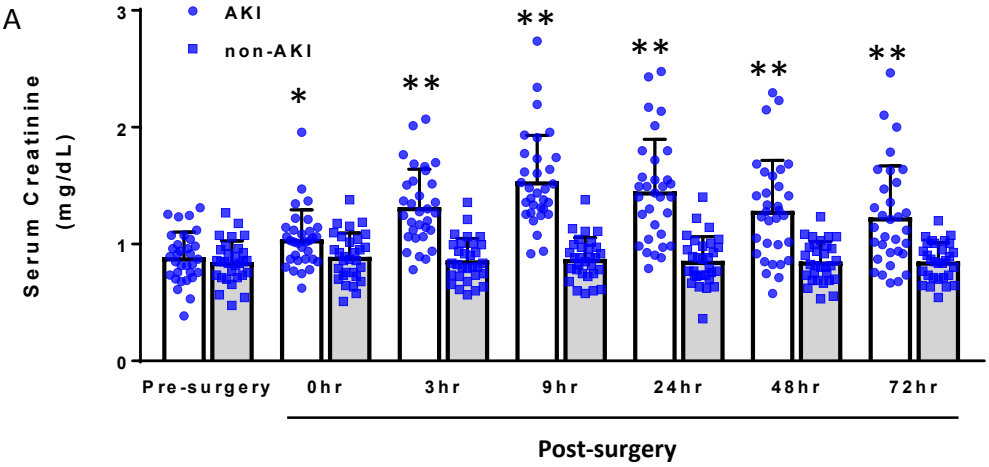

B

Clinical Indexes	Non AKI (n=30)	AKI (n=32)	P Value
Sex	M 20 (66.7%); F 10 (33.3%)	M 22 (68.8%); F 10 (31.3%)	0.8608
Age (year)	59.3±10.1	61.5±9.5	0.3819
Hypertension	8 (26.7%)	9 (28.1%)	0.8976
Diabetes	4 (13.3%)	5 (15.6%)	0.7980
Cerebrovascular disease	1 (8.3%)	2 (6.3%)	0.5928
NYHA>2	25 (83.3%)	29 (90.6%)	0.3921
Contrast medium usage within 1 week before surgery	11 (36.7%)	10 (31.3%)	0.6524
CPB time (minutes)	107.1±14.2	105.4±23.3	0.7284
Aortic cross-clamping time (minutes)	67.4±13.6	64.8±21.4	0.5804
Death rate	0	0	

Supplementary Figure 2 (A) Serum creatinine of cardiopulmonary bypass surgery patients with or without AKI. Serum samples were collected from the patients before surgery or at the indicated time-points after surgery for creatinine measurement (n=30 for non-AKI, n=32 for AKI). *, P<0.05; **, P<0.01; 2-tailed student's t-test between AKI and non-AKI groups. (B) Clinical data of the patients recruited in the study. (Peason's Chi-Square test for Sex, hypertension, diabetes, cerebrovascular disease, NYHA and contrast medium usage difference comparison; 2-tailed student's t-test for all other comparison). NYHA, New York Heart Association Classfication; CPB, cardiopulmonary bypass time.

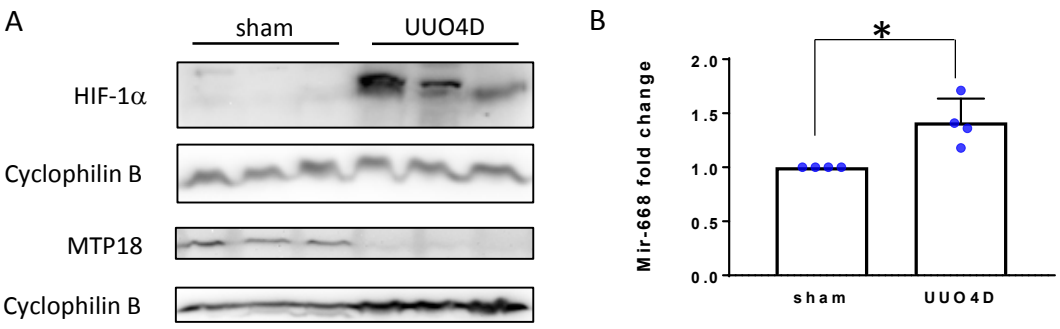

Supplementary Fig. 3 HIF-1 related induction of mir-668 and MTP18 inhibition in unilateral ureteral obstructed kidney. C57BL/6 male mice were subjected to unilateral ureteral obstruction surgery and kept for 4 days (UUO4D). Sham operated mouse kidneys were used for comparison. (A) Immunoblots indicating the induction of HIF-1α and MTP18 suppression in UUO4D kidneys (n=3). Cyclophilin B was used as loading control. (B) qPCR of mir-668 indicating the induction of mir-668 in UUO4D kidneys (n=4, 2-tailed student t-test. *, P=0.0326).

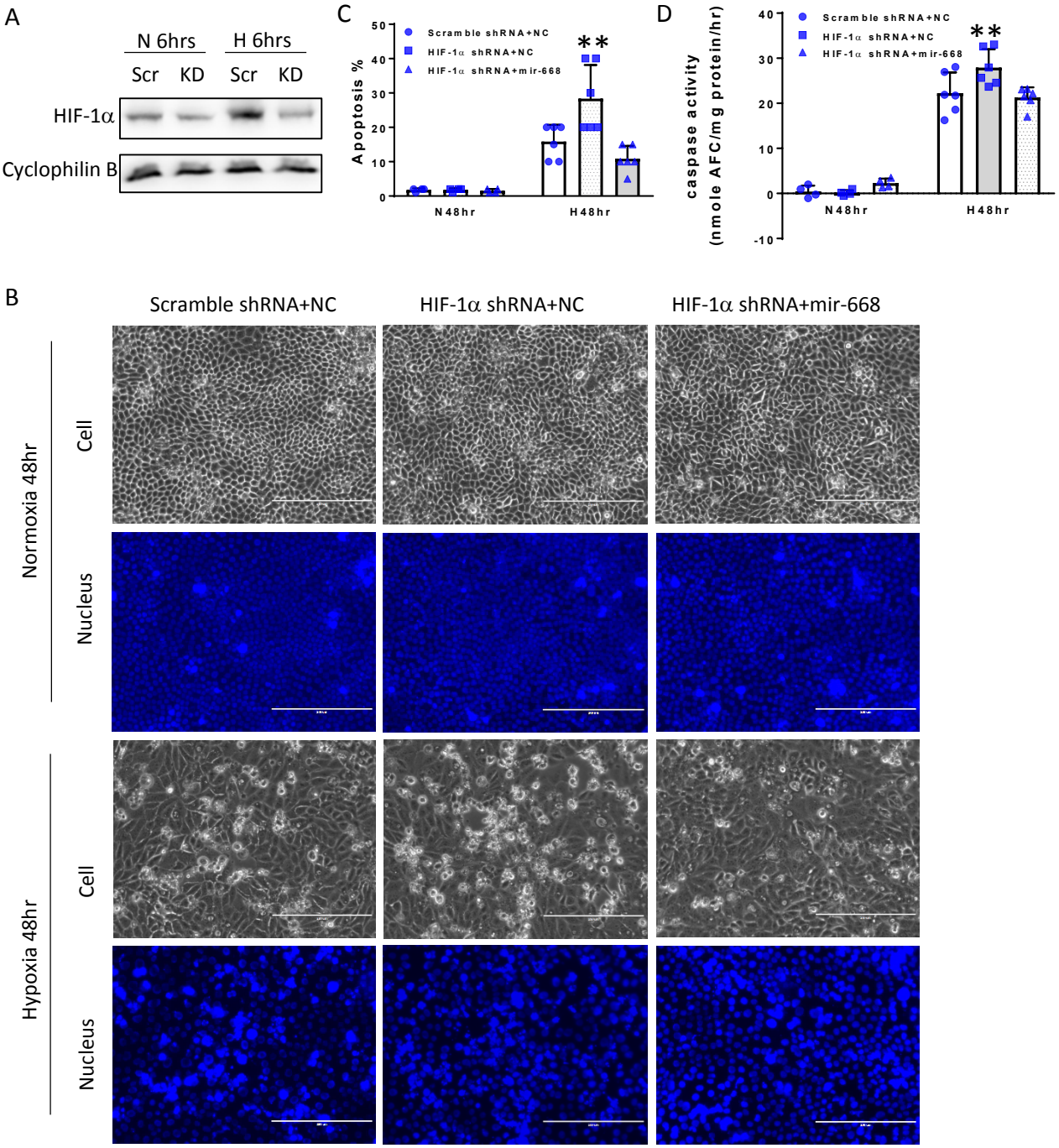

Supplementary Figure 4 Mir-668 reverses HIF-1α deficiency induced induced renal cell apoptosis under hypoxia. RPTC stable cell lines were established with scramble shRNA (Scr) or HIF-1α shRNA (KD) transfection and puromycin selection. The cells were transfected with negative control (NC) or mir-668 mimics and treated with hypoxia. (A) Immunoblots indicating the inhibition of HIF-1α induction by shRNA at 6 hours of normoxia/hypoxia. Cyclophilin B was used as loading control. Experiments were repeated three times. (B) Representative cell and nuclear images showing more apoptosis in HIF-1α knockdown cells after 48 hours of hypoxia treatment and the reverse effect by mir-668 overexpression. (C) Percentage of apoptosis after 48 hours of normoxia/hypoxia. **, P=0.0003, paired one way ANOVA test comparing the hypoxia groups. (D)Caspase activity after 48 hours of normoxia/hypoxia. **, P=0.0080, paired one way ANOVA test comparing the hypoxia groups. n=4 for Normoxia groups, n=6 for hypoxia groups.

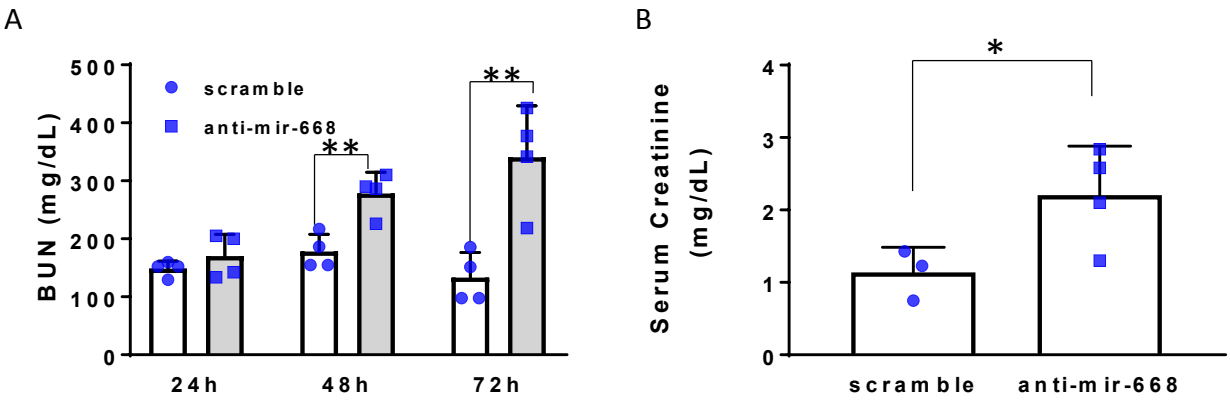

Supplementary Figure 5 Anti-mir-668 worsens AKI induced by 25 minutes of bilateral renal ischemia-reperfusion. Mice were administered with 20mg/kg scramble sequence or anti-mir-668 LNAs 2 days before 25 minutes of bilateral renal ischemia-reperfusion. (A) Significantly higher BUN in anti-mir-668 injected mice at 48 and 72 hours of reperfusion (n=4. **, P=0.0095 for 48h; P=0.0094 for 72h, 2-tailed student's t-test). (B) Significantly higher serum creatinine in anti-mir-668 injected mice at 72 hours of reperfusion (n=3 for scramble and n=4 for anti-mir-668. *, P=0.046, 2-tailed student's t-test).

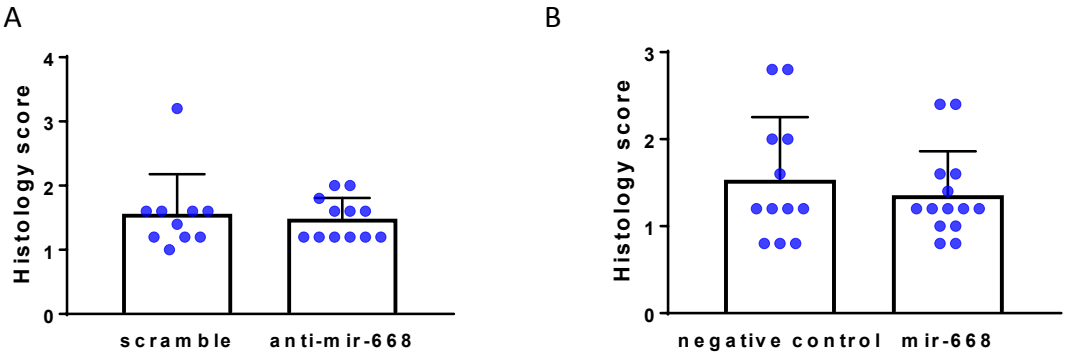

Supplementary Figure 6 mir-668 does not significantly affect histological tubular damage in ischemic AKI. Histological tubular damage was assessed following hematoxylin and eosin staining. The injury was scaled from 0-4 according to the estimation of the percentage from 0-100%. (A) Effect of anti-mir-668-LNA on histological tubular damage induced by 28 minutes of bilateral kidney ischemia and 48 hours of reperfusion (n=10 for left and right kidneys respectively from scramble group, n=12 for left and right kidneys respectively from anti-mir-668 group). (B) Effect of mir-668 mimic on histological tubular damage induced by 30 minutes of bilateral renal ischemia with 48 hours of reperfusion (n=12 for left and right kidneys respectively from negative control group, n=14 for left and right kidneys respectively from mir-668 group).

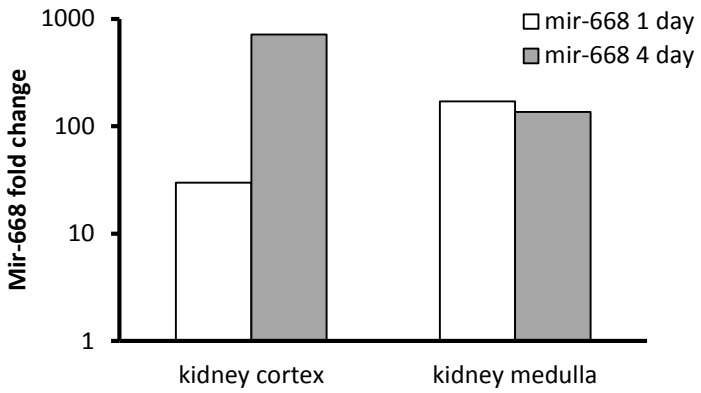

Supplementary Figure 7 Quantitative real time PCR showing mir-668 increases in kidneys after mir-668 mimic administration comparing to negative controls (n=1). Negative control or mir-668 mimic oligos were delivered to C57BL/6J male mice through tail vein injection to collect kidney cotex and medulla tissues at 1 day or 4 days for qPCR assay.

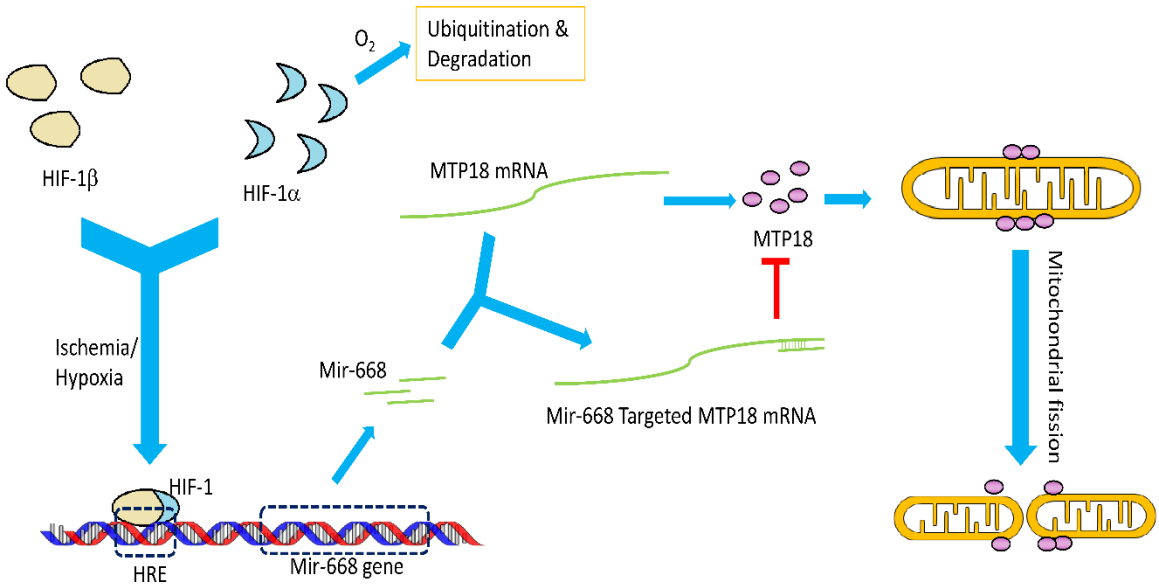

Supplementary Figure 8 Schematic diagram of the HIF-1/mir-668/MTP18 pathway in mitochondrial regulation. Under ischemia/hypoxia, HIF-1α is stabilized to associate with HIF-1β, forming the functional dimer of HIF-1. HIF-1 then translocates into the nucleus and binds to hypoxia-responsive elements (HRE) leading to the transcription of relevant genes, such as mir-668. mir-668 can bind to MTP18 mRNA to repress the translation and expression of MTP18 (a mitochondrial fission protein) resulting in the prevention of mitochondrial fragmentation.

Supplementary Table 1 Protein-coding genes with their mRNAs pulled down in mir-668 miRISC. HEK293 cells were transfected with negative control (NC) and mir-668 mimics (mir-668). The miRISC complex was precipitated by Ago 2 antibodies followed by RNA-seq. The precipitated mRNAs with over 2 fold increase in mir-668 group (vs. NC) were identified, of which 124 having miR-668–targeting seed sequence are listed. They are categorized by their fold change in total RNAs from mir-668 group vs NC group.

668 total/NC total<0.8 (25 genes)	0.8<668 total/NC total<2 (71 genes)			668 total/NC total>2 (28 genes)	
SHD	DNALI1	SLC26A1	CD4	IFI44L	KCNK3
KLHL30	HES2	POU2F2	INPP5D	FUT3	NOVA2
LAIR1	CTNNBIP1	ZC3H12B	SCARA5	PCSK2	STK32B
C9orf85	PKD1L2	SLC17A7	PELI3	SMOC2	
LRRC32	APBA1	MICA	KIAA1199	ZFP3	
C22orf24	FGD3	SHANK2	KCNA1	CHODL	
GPR61	OAS2	MTFP1, SEC14L2	CSMD2	RSAD2	
AQP4	SCUBE2	MDGA1	MGLL	GBP1	
RGSL1	LRRC2	C3orf15	KNDC1	LRP1B	
GDF9	FAM57B	TMEM155	IGSF11	SLC6A12	
FAT2	ATP8B3	B3GAT3	CUX2	DACT2	
NFASC	ROM1	SAMD12	CDH1	DIO2	
B9D2	RHEBL1	PLXNB3, SPRK3	CDH13	GABBR2	
SHROOM4	FMN1	ALDH1A1	SLC15A1	HS3ST1	
PPEF1	BMP8A	ANKRD20A4	SLC9A9	C6orf97	
TEC	GCK	ZNF805	FAM182A	GLRA2	
C19orf52	RAB40C	PRDM16	PDE4C	ZNF626	
TST	TNFRSF8	TNFSF10	SHISA7	CYLC2	
ZNF347	PTPRN2	ALDH1L2	IGFN1	PCDH11Y	
GPR146	COL7A1	IL22RA1		MC2R	
OLIG1	KCNQ2	DNAH10		APOL1	
ECHDC3	XKRX	RASD2		CD3G	
TNFSF4	PPM1H	KLRG1		HHLA1	
ST6GALNAC5	TTBK1	MYOZ3		IKZF1	
RELN	SHC4	C5AR1		KCNJ5	

Supplementary Table 2 List of potential mir-668 binding sites in 3'-UTR of MTP18 gene (MTFP1) predicted by Segal Lab computation. (A) The predicted sites for human gene. 1, 2, the top two sites examined by luciferase analysis. (B) The predicted sites for mouse gene. (C) The predicted sites for rat gene. DGduplex, the free energy gained by the binding of the microRNA to the target. DGopen, the free energy lost by unpairing the target-site nucleotides. DDG, the difference between DGduplex and DGopen.

A

Gene	microRNA	Position	Seed	ΔGduplex	ΔGopen	ΔΔG
MTFP1-001 utr3:KNOWN_protein_coding[1]	hsa-miR-668-3p MIMAT0003881	139	6:1:0	-24	-9.31	-14.68
MTFP1-001 utr3:KNOWN_protein_coding[2]	hsa-miR-668-3p MIMAT0003881	414	7:1:1	-20.9	-10.26	-10.63
MTFP1-001 utr3:KNOWN_protein_coding	hsa-miR-668-3p MIMAT0003881	236	6:1:1	-18.6	-11.13	-7.46
MTFP1-001 utr3:KNOWN_protein_coding	hsa-miR-668-3p MIMAT0003881	161	6:0:1	-14.4	-8.55	-5.84
MTFP1-001 utr3:KNOWN_protein_coding	hsa-miR-668-3p MIMAT0003881	229	7:1:1	-17.6	-12.43	-5.16
MTFP1-001 utr3:KNOWN_protein_coding	hsa-miR-668-3p MIMAT0003881	173	7:1:0	-16.6	-11.94	-4.65
MTFP1-001 utr3:KNOWN_protein_coding	hsa-miR-668-3p MIMAT0003881	383	7:1:0	-15.87	-12.28	-3.58
MTFP1-001 utr3:KNOWN_protein_coding	hsa-miR-668-3p MIMAT0003881	456	6:1:0	-11.1	-13.5	2.4
MTFP1-001 utr3:KNOWN_protein_coding	hsa-miR-668-3p MIMAT0003881	89	6:1:1	-15	-19.84	4.84
MTFP1-001 utr3:KNOWN_protein_coding	hsa-miR-668-3p MIMAT0003881	299	7:1:0	-11.8	-16.87	5.07

B

Gene	microRNA	Position	Seed	ΔGduplex	ΔGopen	ΔΔG
Mtfp1-001 utr3:KNOWN_protein_coding	mmu-miR-668-3p MIMAT0003732	593	7:1:0	-24.1	-10.41	-13.68
Mtfp1-001 utr3:KNOWN_protein_coding	mmu-miR-668-3p MIMAT0003732	114	6:1:1	-21.2	-9.1	-12.09
Mtfp1-001 utr3:KNOWN_protein_coding	mmu-miR-668-3p MIMAT0003732	197	7:1:1	-24.9	-12.81	-12.08
Mtfp1-001 utr3:KNOWN_protein_coding	mmu-miR-668-3p MIMAT0003732	136	6:0:1	-20.26	-8.84	-11.41
Mtfp1-001 utr3:KNOWN_protein_coding	mmu-miR-668-3p MIMAT0003732	535	6:1:0	-19.4	-8.46	-10.93
Mtfp1-001 utr3:KNOWN_protein_coding	mmu-miR-668-3p MIMAT0003732	542	6:1:0	-15.61	-5.32	-10.28
Mtfp1-001 utr3:KNOWN_protein_coding	mmu-miR-668-3p MIMAT0003732	55	6:1:1	-19.73	-10.04	-9.68
Mtfp1-001 utr3:KNOWN_protein_coding	mmu-miR-668-3p MIMAT0003732	715	6:1:1	-15.86	-7.2	-8.65
Mtfp1-001 utr3:KNOWN_protein_coding	mmu-miR-668-3p MIMAT0003732	688	6:1:1	-23.2	-15.75	-7.44
Mtfp1-001 utr3:KNOWN_protein_coding	mmu-miR-668-3p MIMAT0003732	179	6:0:1	-22.42	-17.86	-4.55
Mtfp1-001 utr3:KNOWN_protein_coding	mmu-miR-668-3p MIMAT0003732	585	7:1:1	-15.25	-13.15	-2.09
Mtfp1-001 utr3:KNOWN_protein_coding	mmu-miR-668-3p MIMAT0003732	142	6:1:0	-14.9	-13.03	-1.86
Mtfp1-001 utr3:KNOWN_protein_coding	mmu-miR-668-3p MIMAT0003732	691	7:1:1	-22.3	-20.58	-1.71
Mtfp1-001 utr3:KNOWN_protein_coding	mmu-miR-668-3p MIMAT0003732	268	6:1:1	-5.2	-3.85	-1.34
Mtfp1-001 utr3:KNOWN_protein_coding	mmu-miR-668-3p MIMAT0003732	100	6:1:1	-13.2	-12.74	-0.45
Mtfp1-001 utr3:KNOWN_protein_coding	mmu-miR-668-3p MIMAT0003732	741	6:1:1	-4.4	-4.33	-0.069
Mtfp1-001 utr3:KNOWN_protein_coding	mmu-miR-668-3p MIMAT0003732	351	6:1:1	-14.6	-15.91	1.31
Mtfp1-001 utr3:KNOWN_protein_coding	mmu-miR-668-3p MIMAT0003732	416	6:1:1	-12.96	-16.22	3.26
Mtfp1-001 utr3:KNOWN_protein_coding	mmu-miR-668-3p MIMAT0003732	570	6:1:0	-12.26	-18.34	6.08

C

Gene	microRNA	Position	Seed	ΔGduplex	ΔGopen	ΔΔG
Mtfp1-201 utr3:KNOWN_protein_coding	rno-miR-668 MIMAT0012839	698	6:1:1	-18.9	-6.15	-12.74
Mtfp1-201 utr3:KNOWN_protein_coding	rno-miR-668 MIMAT0012839	673	8:1:1	-28.1	-16.9	-11.19
Mtfp1-201 utr3:KNOWN_protein_coding	rno-miR-668 MIMAT0012839	179	7:1:1	-28	-18.76	-9.23
Mtfp1-201 utr3:KNOWN_protein_coding	rno-miR-668 MIMAT0012839	123	6:1:0	-21.01	-13	-8
Mtfp1-201 utr3:KNOWN_protein_coding	rno-miR-668 MIMAT0012839	523	6:1:0	-15.45	-8.98	-6.46
Mtfp1-201 utr3:KNOWN_protein_coding	rno-miR-668 MIMAT0012839	567	6:1:1	-17.42	-11.3	-6.11
Mtfp1-201 utr3:KNOWN_protein_coding	rno-miR-668 MIMAT0012839	193	6:1:1	-18	-12.04	-5.95
Mtfp1-201 utr3:KNOWN_protein_coding	rno-miR-668 MIMAT0012839	559	6:1:1	-17.15	-11.53	-5.61
Mtfp1-201 utr3:KNOWN_protein_coding	rno-miR-668 MIMAT0012839	55	6:1:1	-17.64	-12.93	-4.7
Mtfp1-201 utr3:KNOWN_protein_coding	rno-miR-668 MIMAT0012839	94	6:1:1	-12.6	-8.41	-4.18
Mtfp1-201 utr3:KNOWN_protein_coding	rno-miR-668 MIMAT0012839	23	7:1:1	-15.3	-12.75	-2.54
Mtfp1-201 utr3:KNOWN_protein_coding	rno-miR-668 MIMAT0012839	574	7:1:0	-15.6	-13.28	-2.31
Mtfp1-201 utr3:KNOWN_protein_coding	rno-miR-668 MIMAT0012839	724	6:1:1	-4.4	-2.8	-1.59
Mtfp1-201 utr3:KNOWN_protein_coding	rno-miR-668 MIMAT0012839	161	6:0:1	-17.99	-16.46	-1.52
Mtfp1-201 utr3:KNOWN_protein_coding	rno-miR-668 MIMAT0012839	551	6:1:0	-13.84	-12.44	-1.39
Mtfp1-201 utr3:KNOWN_protein_coding	rno-miR-668 MIMAT0012839	393	6:1:1	-16.55	-15.3	-1.24
Mtfp1-201 utr3:KNOWN_protein_coding	rno-miR-668 MIMAT0012839	249	6:1:1	-5.7	-6.1	0.4
Mtfp1-201 utr3:KNOWN_protein_coding	rno-miR-668 MIMAT0012839	116	6:1:1	-16.45	-17.2	0.75
Mtfp1-201 utr3:KNOWN_protein_coding	rno-miR-668 MIMAT0012839	296	6:1:1	-6.4	-8.14	1.74
Mtfp1-201 utr3:KNOWN_protein_coding	rno-miR-668 MIMAT0012839	448	6:1:1	-10.31	-14.25	3.94
Mtfp1-201 utr3:KNOWN_protein_coding	rno-miR-668 MIMAT0012839	328	6:1:1	-8.01	-13.32	5.31

Full unedited blot for Figure 1A

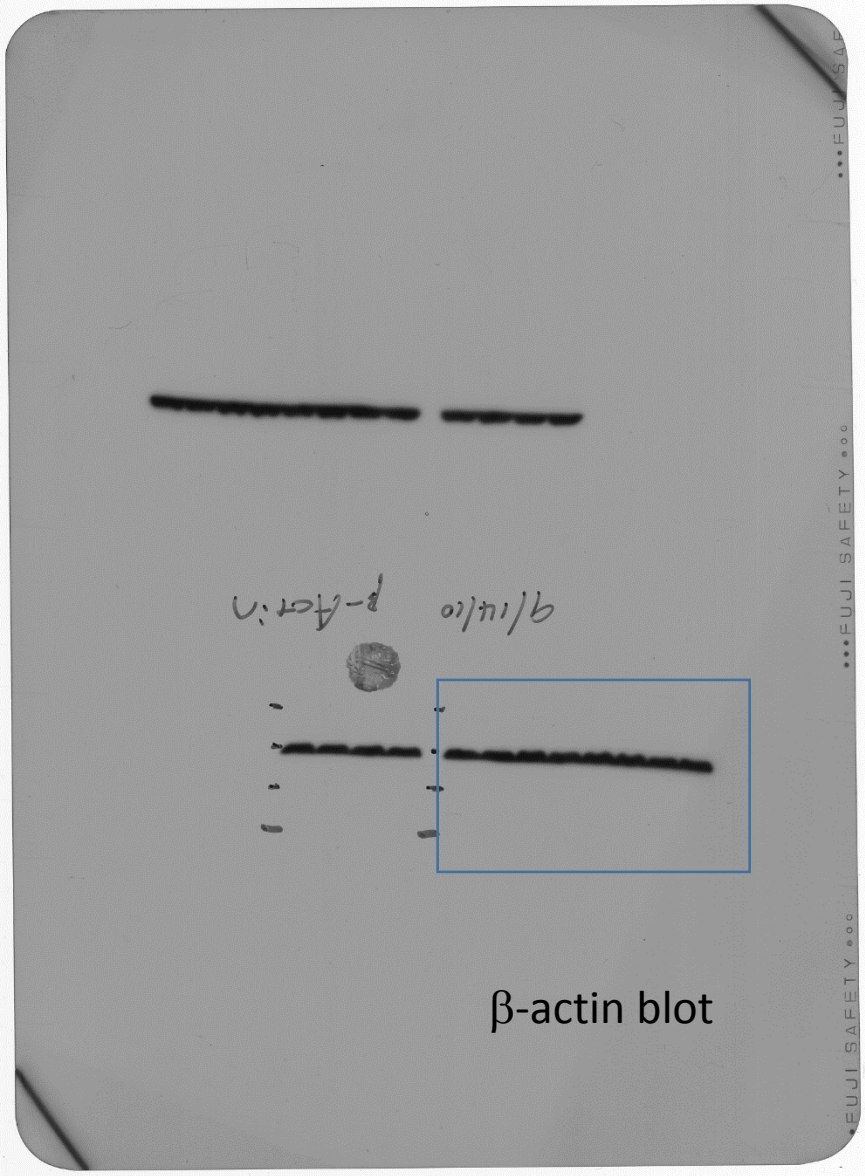

HIF-1α blot

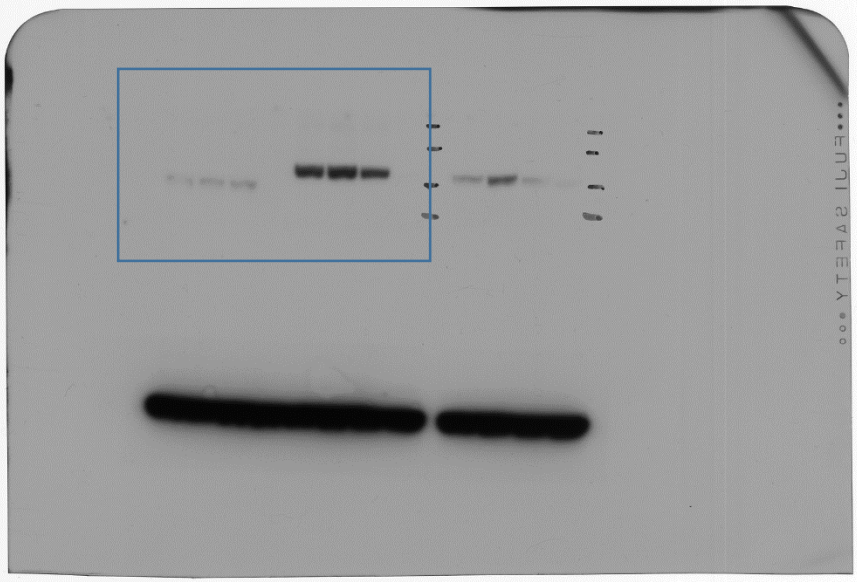

Full images for Figure 4H

Cyclophilin b blot

Picture of PVDF membrane

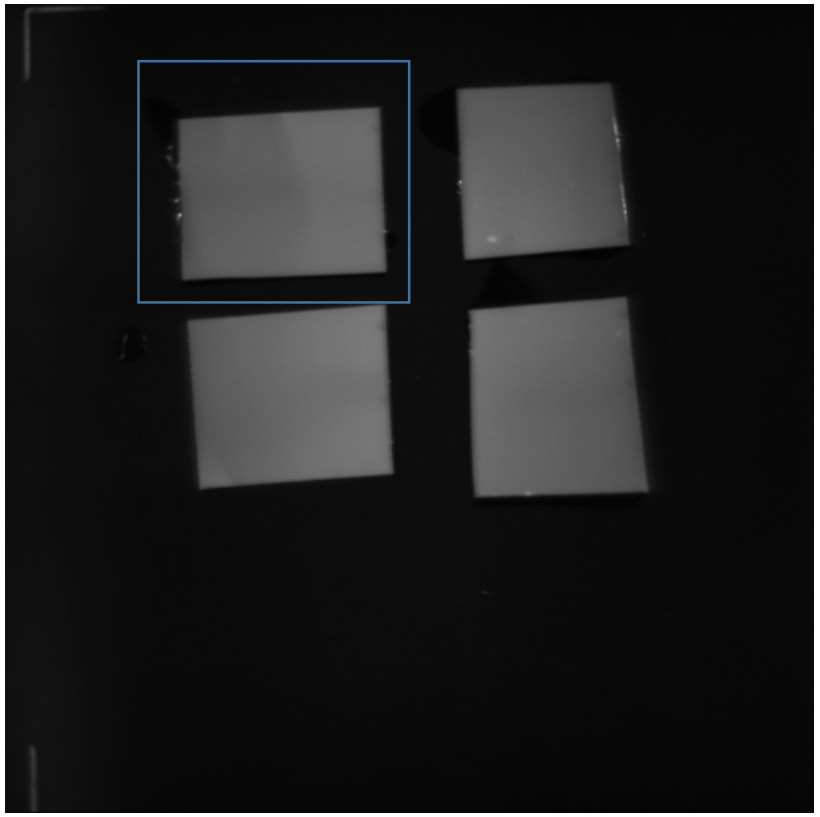

Full images for Figure 4H

Active caspase 3 blot

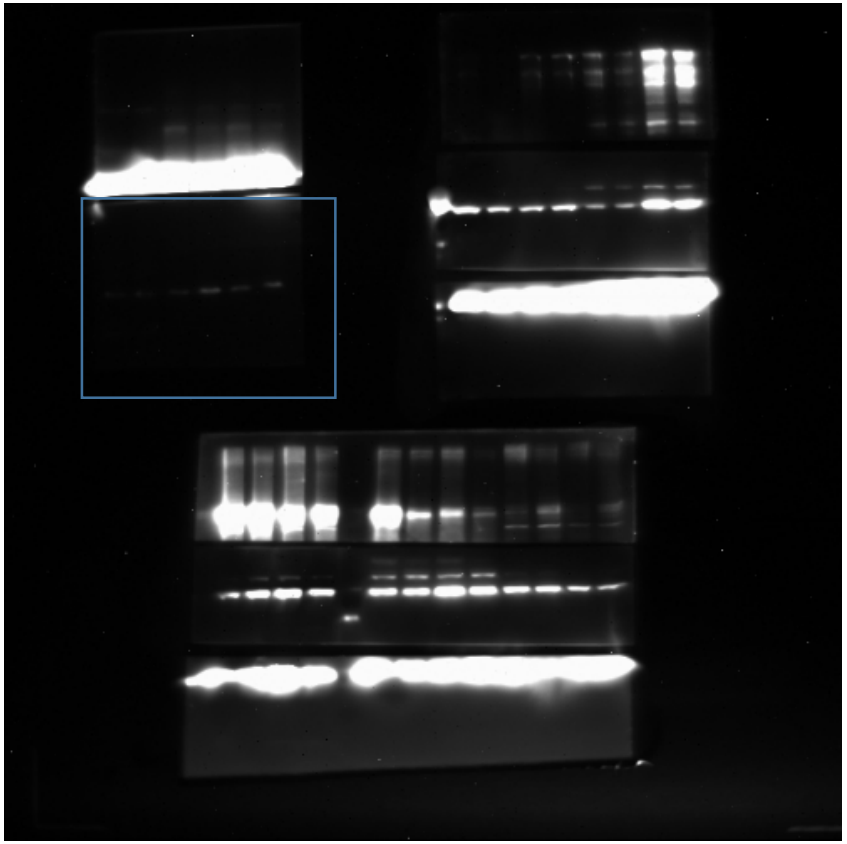

Picture of PVDF membrane

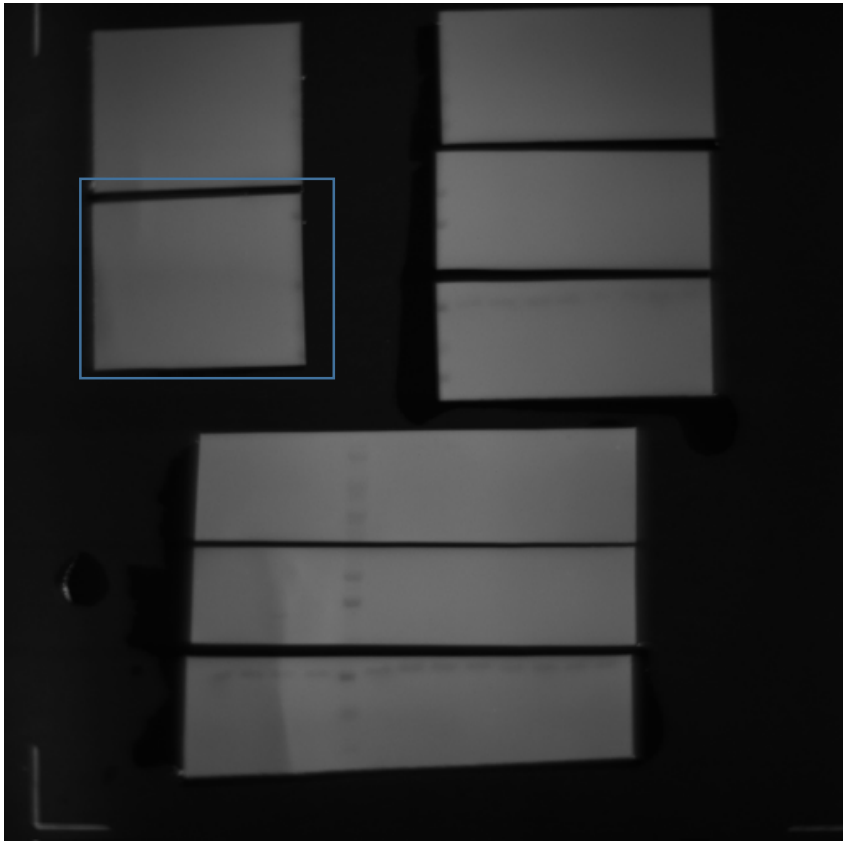

Full images for Figure 5H

Active caspase 3 blot

Picture of PVDF membrane

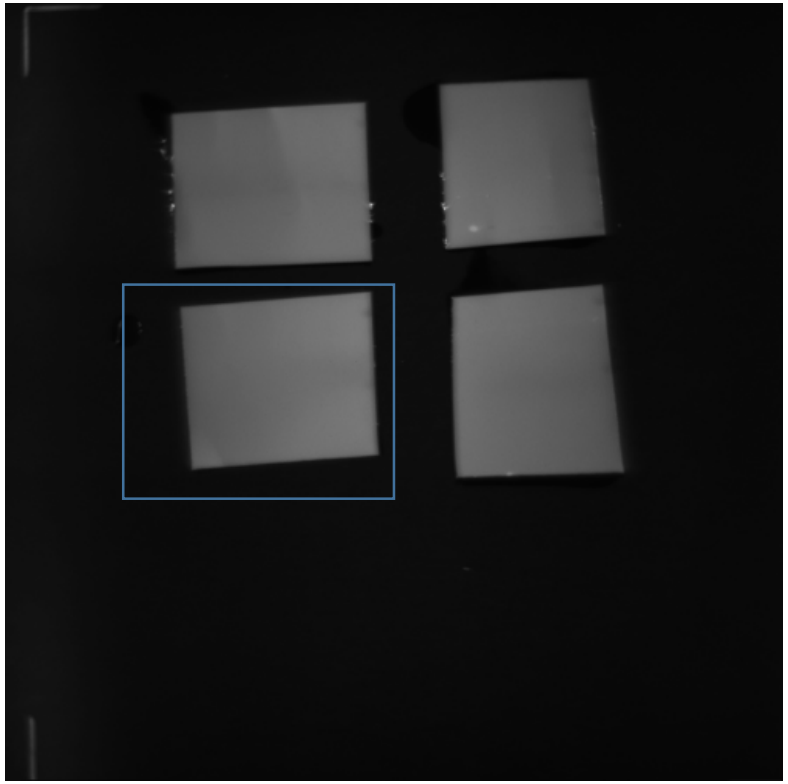

Full images for Figure 5H

Cyclophilin b blot

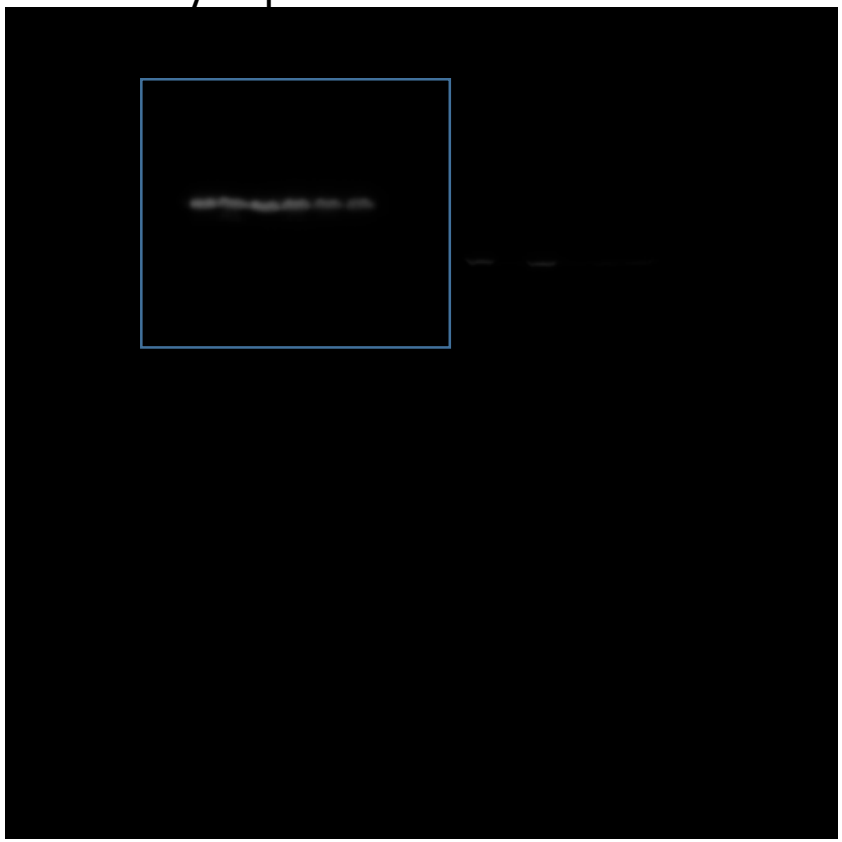

Picture of PVDF membrane

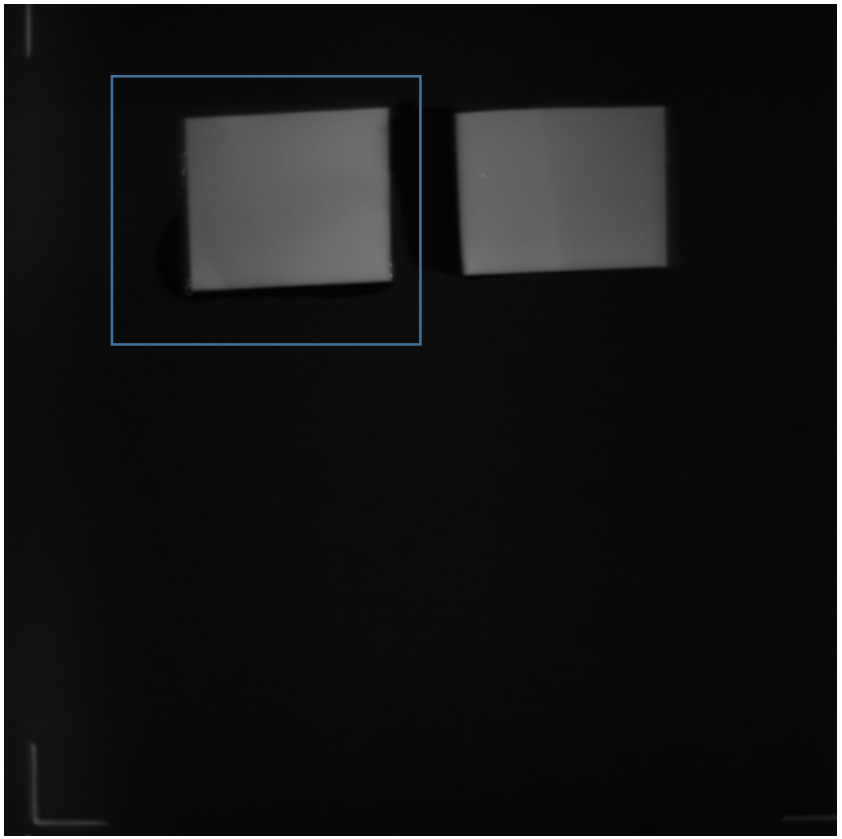

Full images for Figure 6E

Blot for Bak

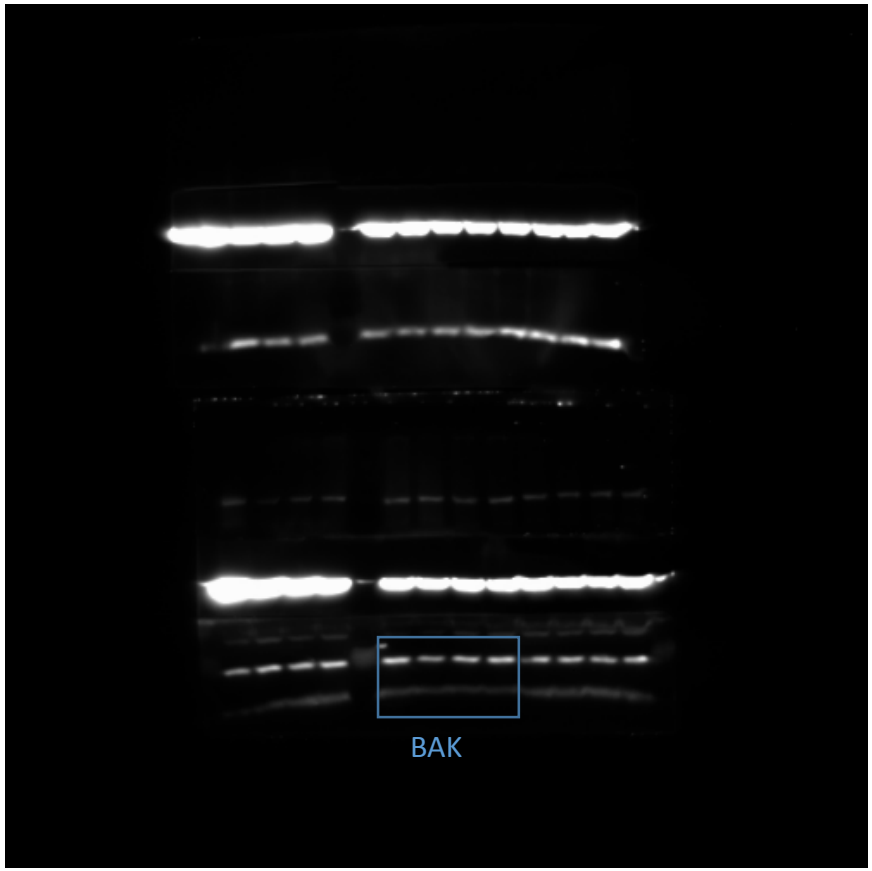

Picture of PVDF membrane

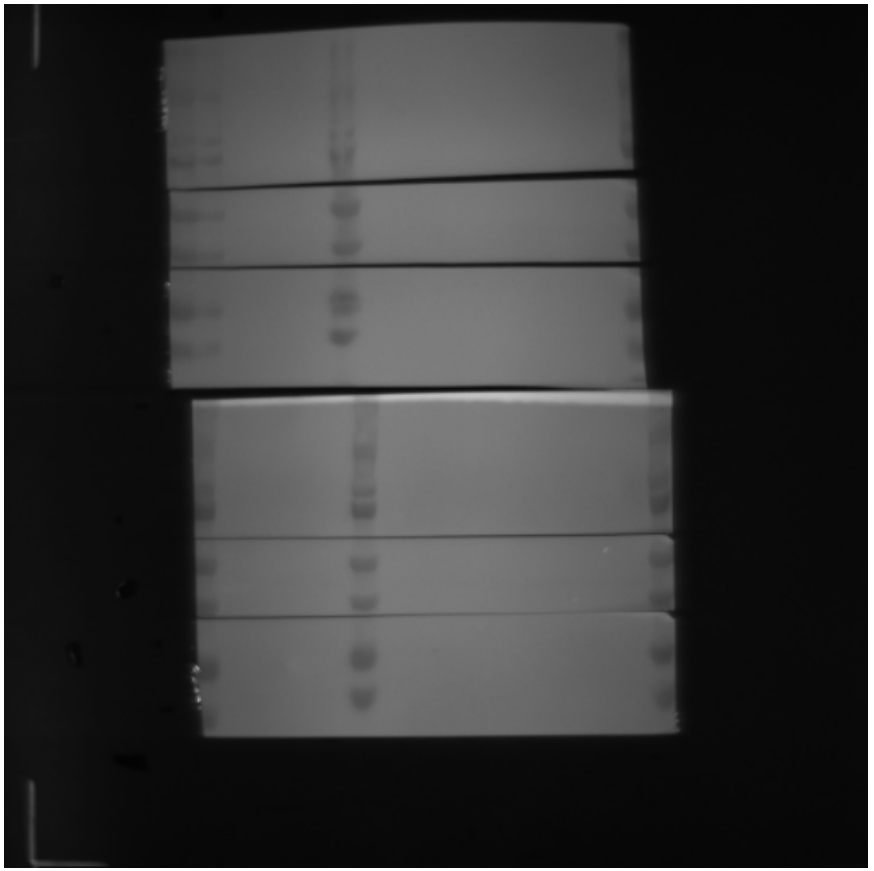

Full images for Figure 6E

Blot for p-Drp1(S-637)

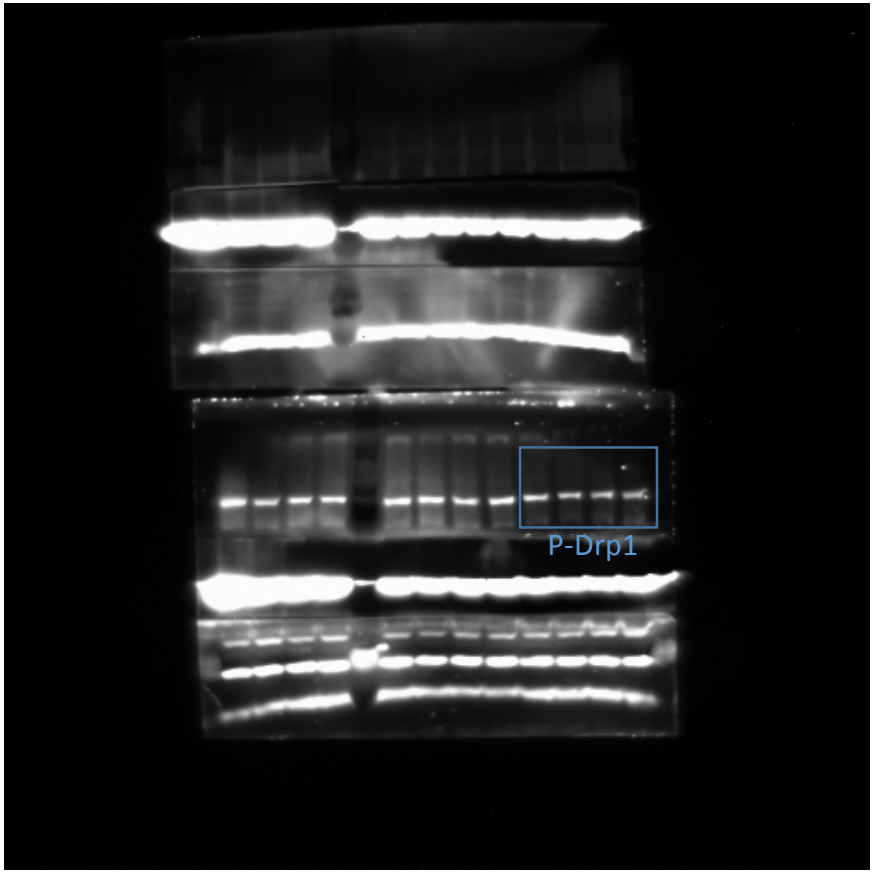

Picture of PVDF membrane

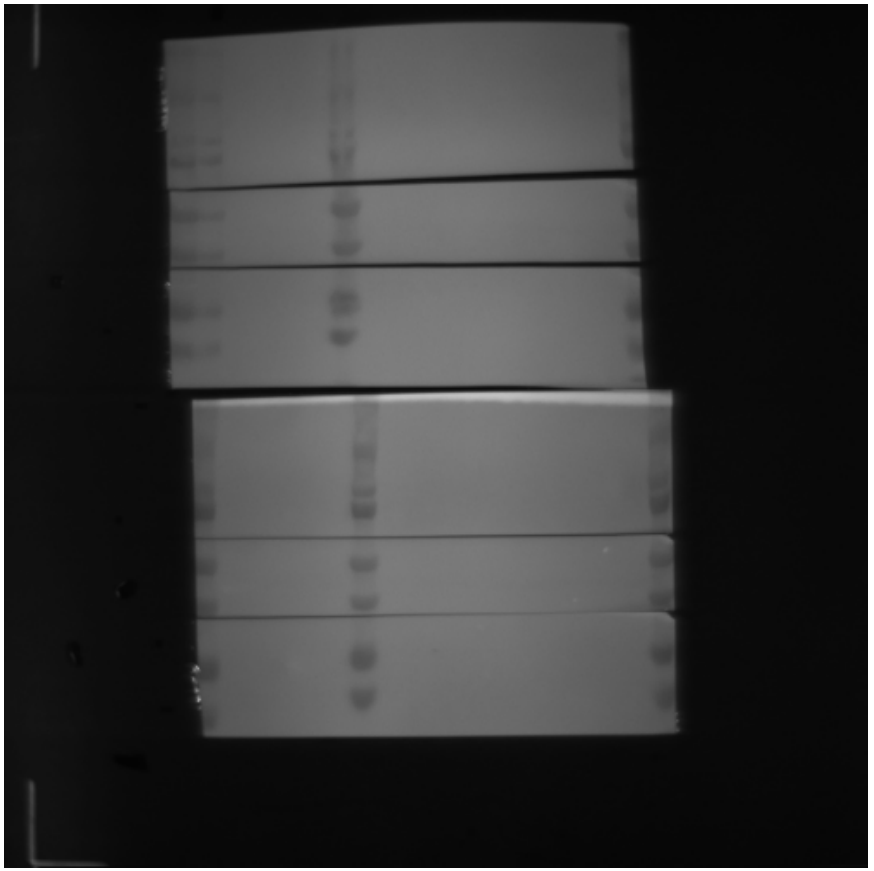

Full images for Figure 6E

Blots for β-actin

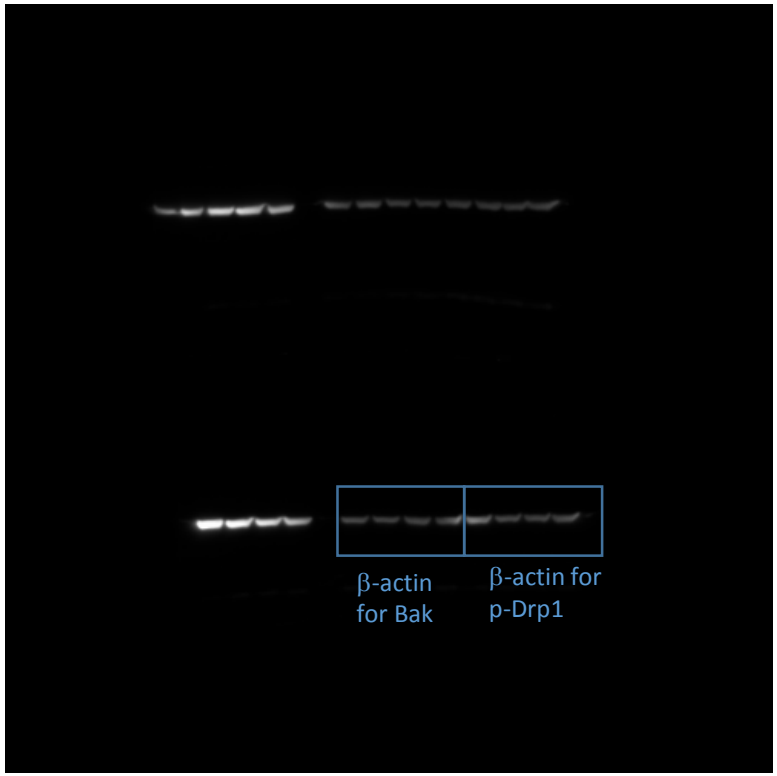

Picture of PVDF membrane

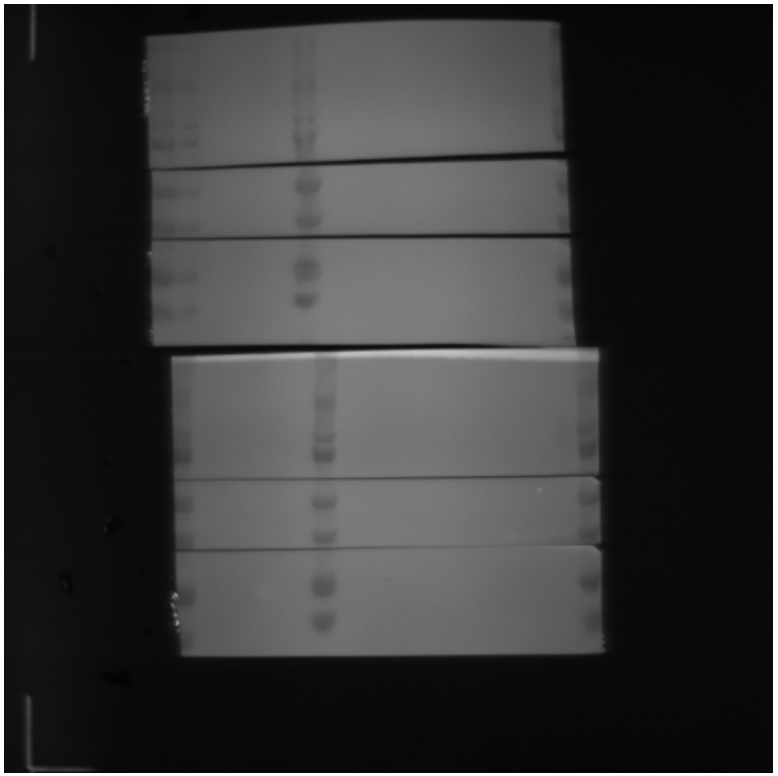

Full images for Figure 6E

Blots for Drp1 and β-actin

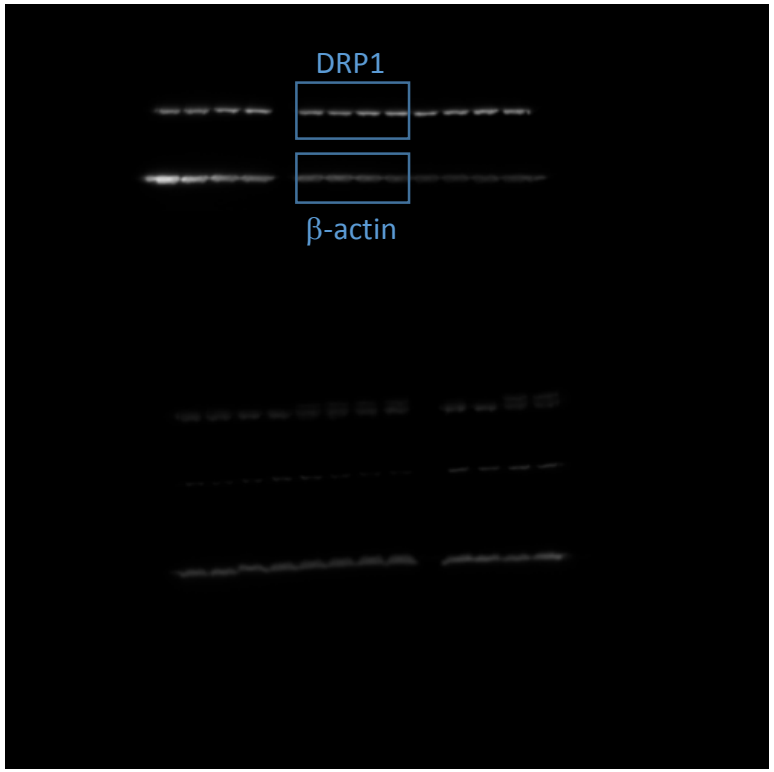

Picture of PVDF membrane

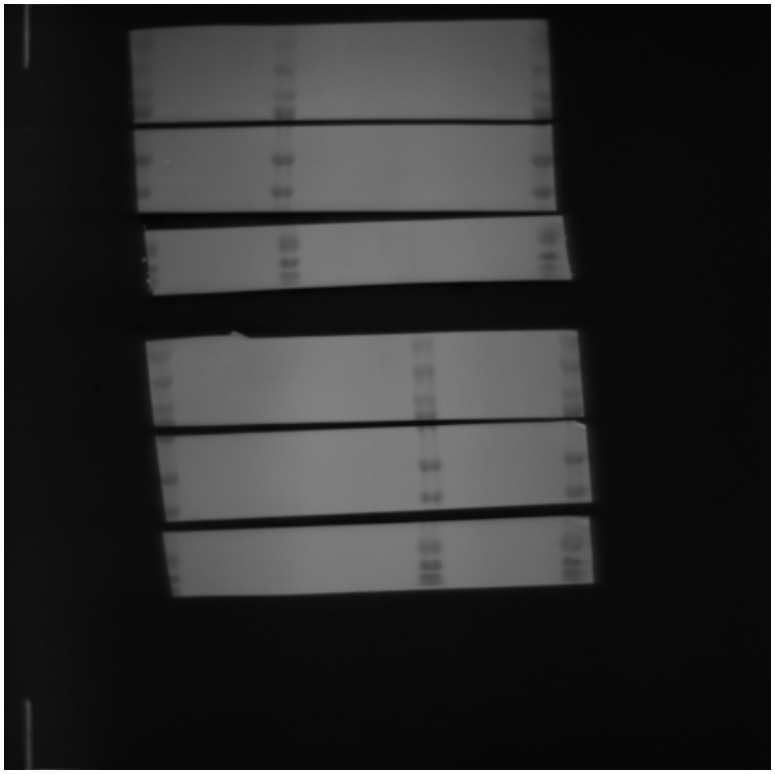

Full images for Figure 6E

Blots for OPA1, OMA1, Cyclophilin B

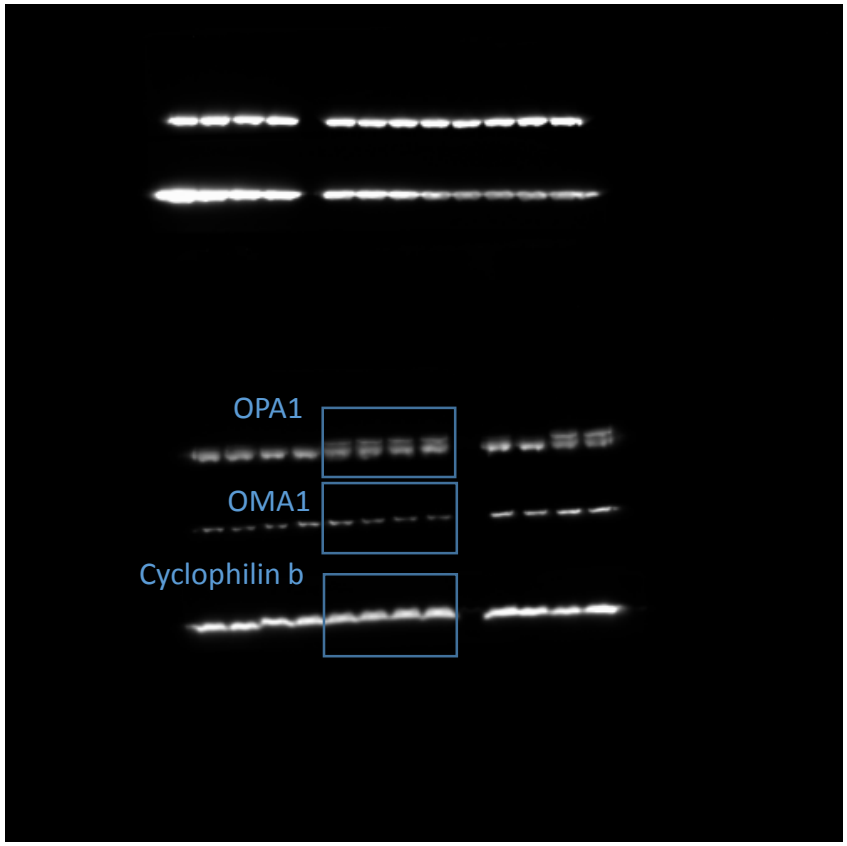

Picture of PVDF membrane

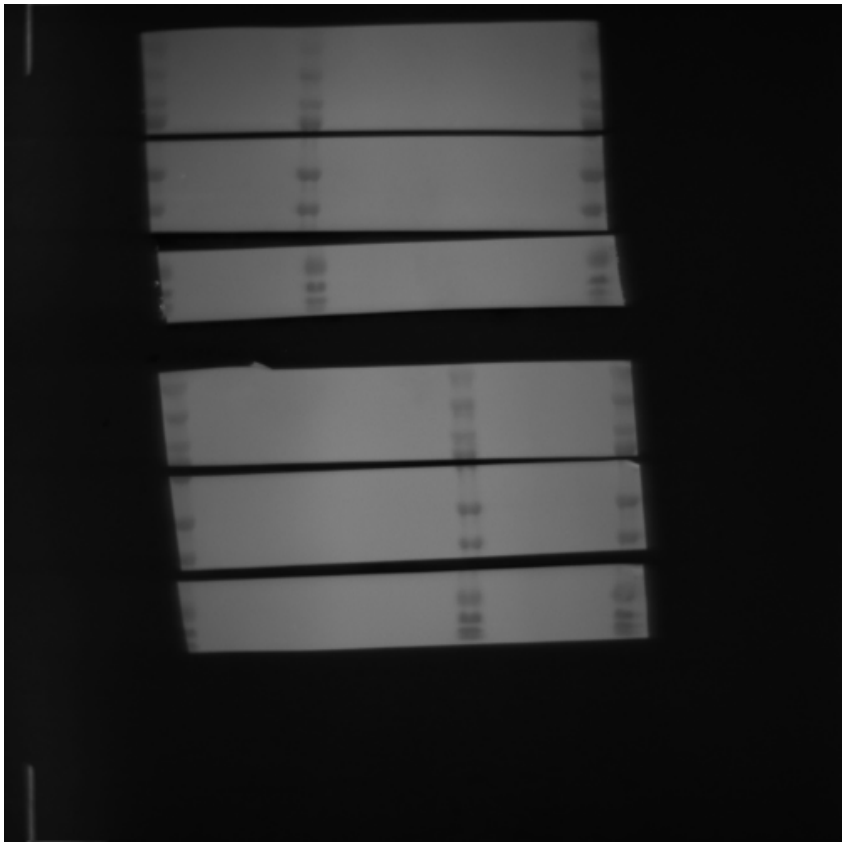

Full images for Figure 6E

Blot for MFN2

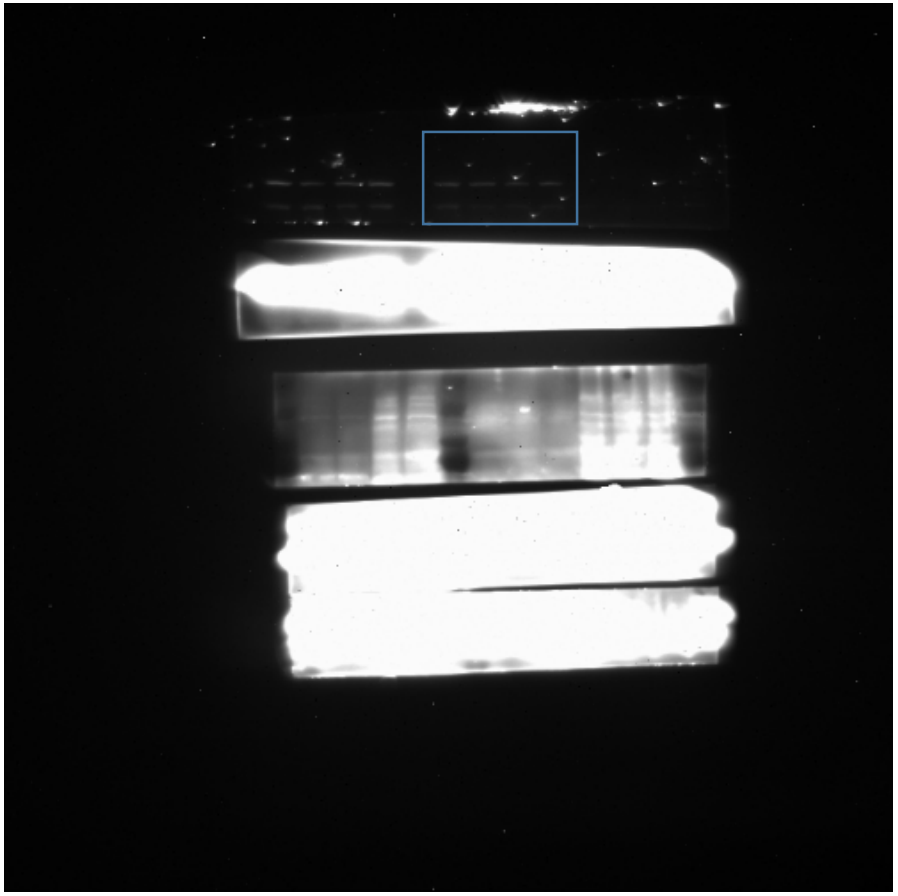

Picture of PVDF membrane

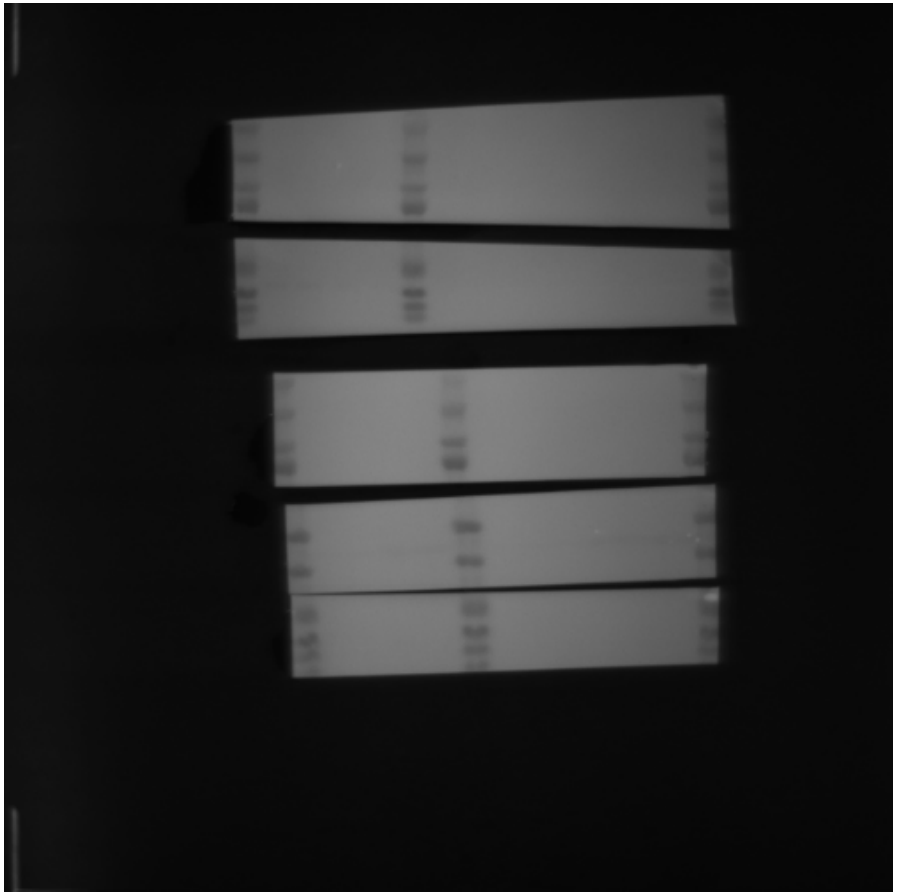

Full images for Figure 6E

Blot for cyclophilin b (MFN2)

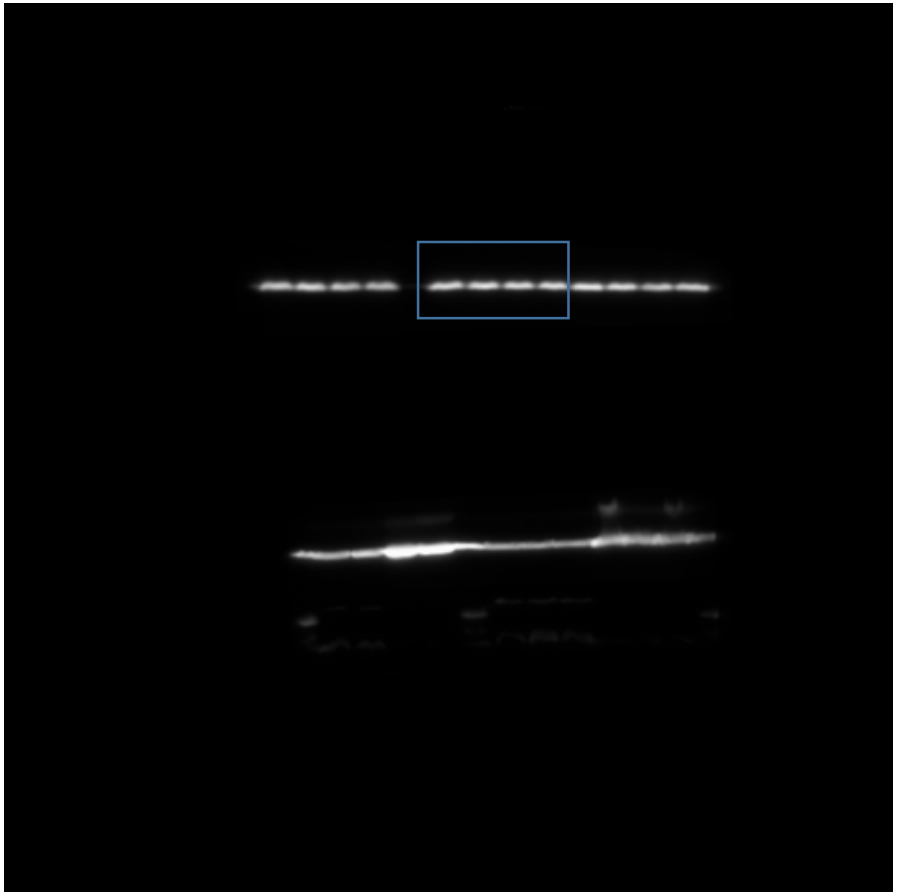

Picture of PVDF membrane

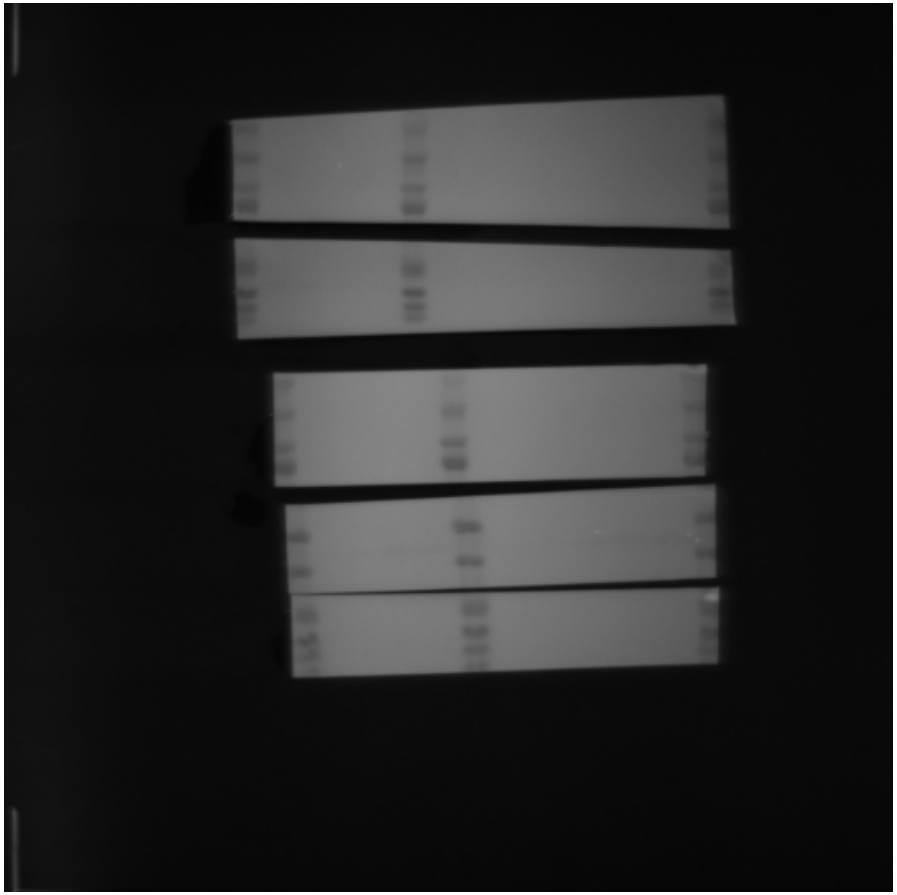

Full unedited blot for Figure 6E MFN1

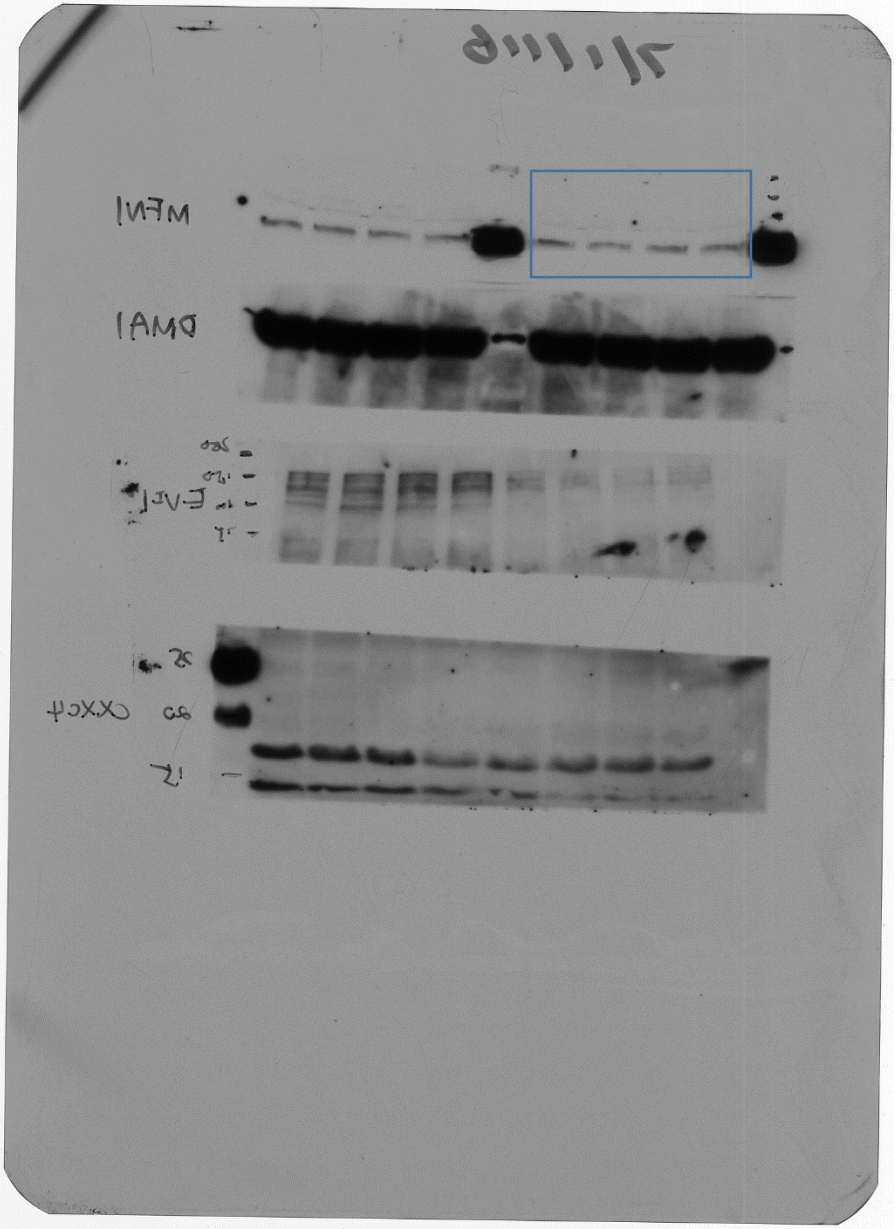

Full images for Figure 6E

Blot for cyclophilin b (MFN1)

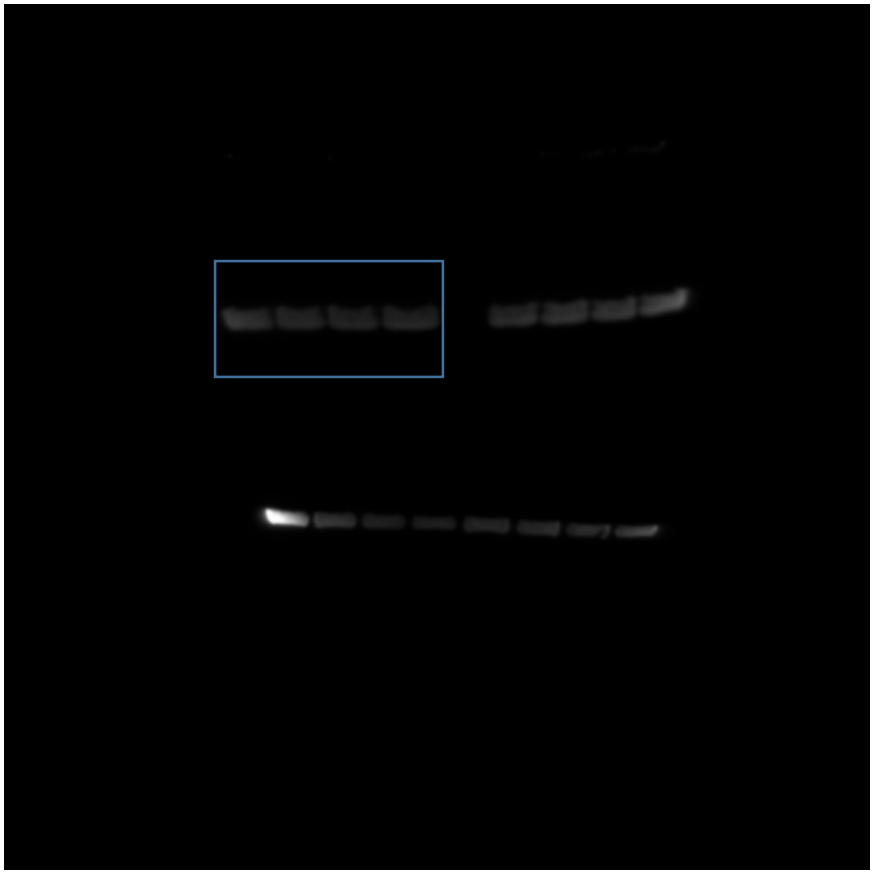

Picture of PVDF membrane

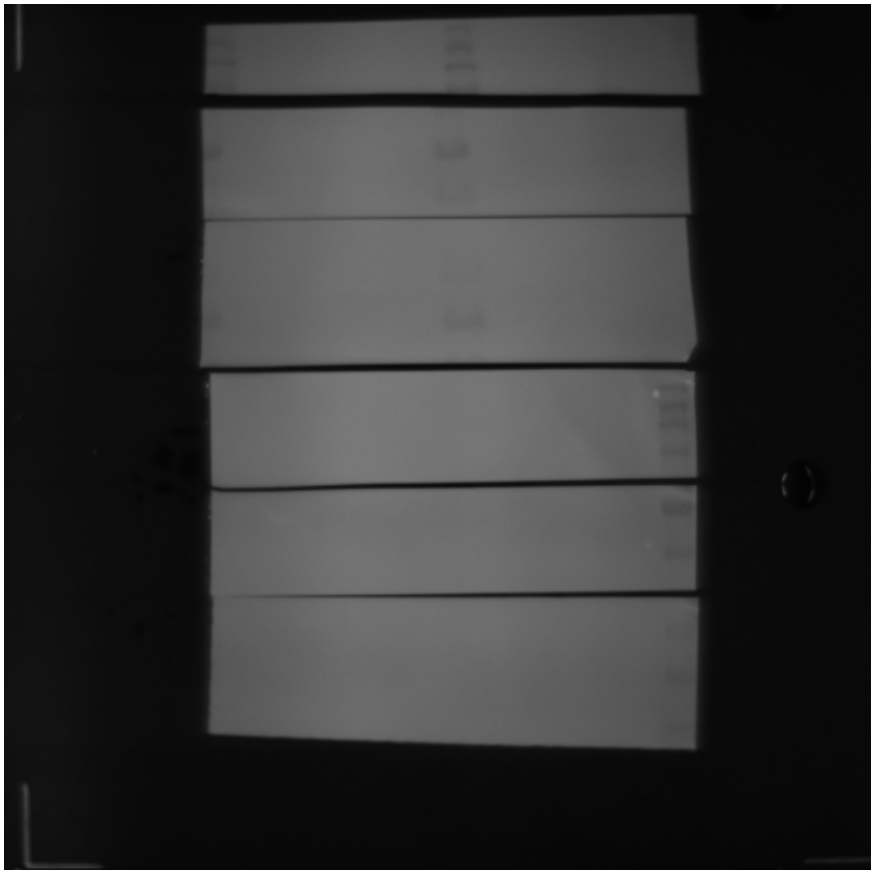

Full images for Figure 7B and Figure 7C

Blot for MTP18

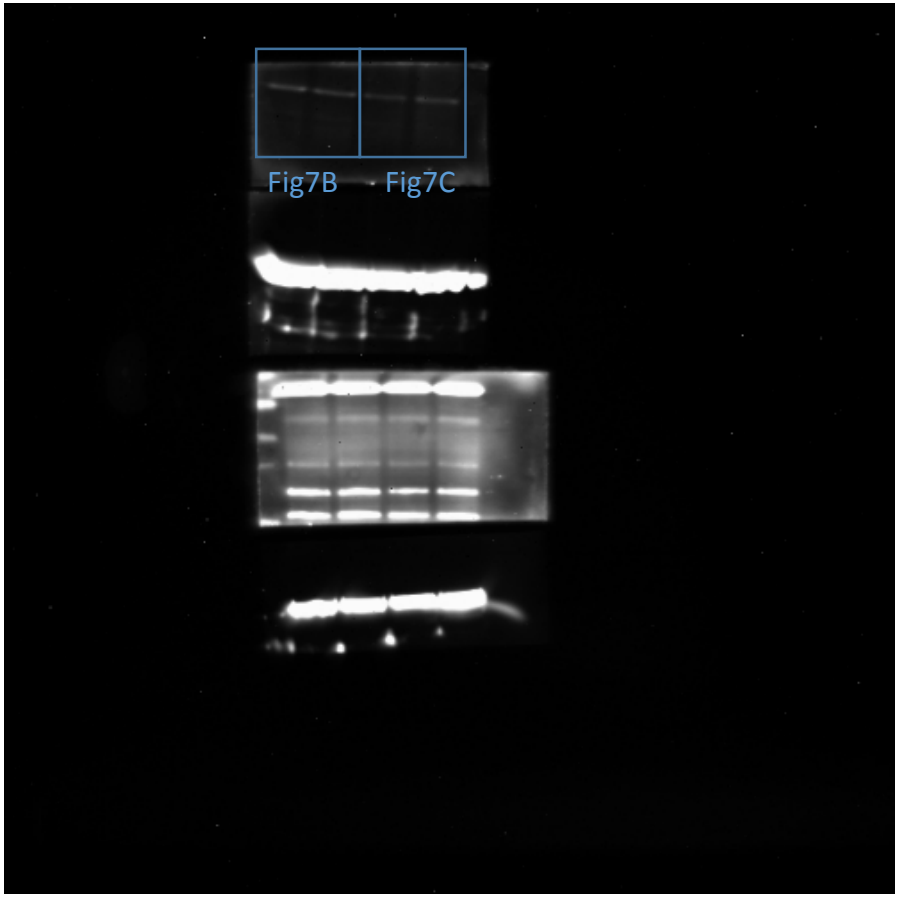

Picture of PVDF membrane

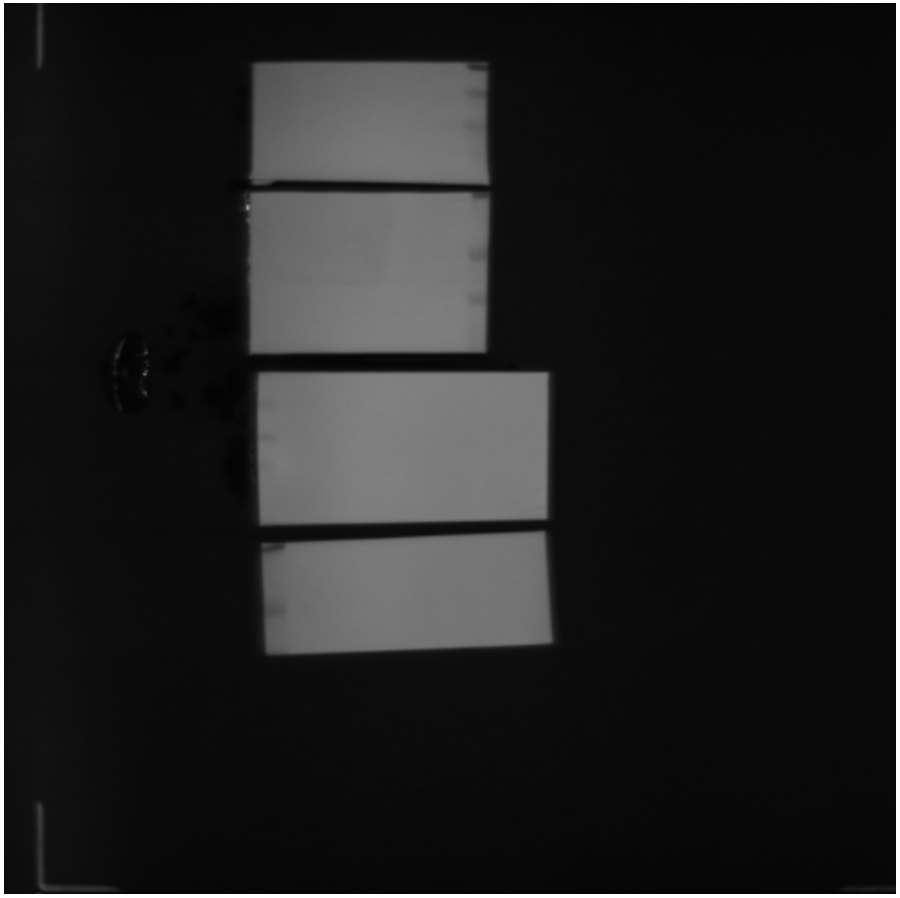

Full images for Figure 7B and Figure 7C

Blot for β-actin

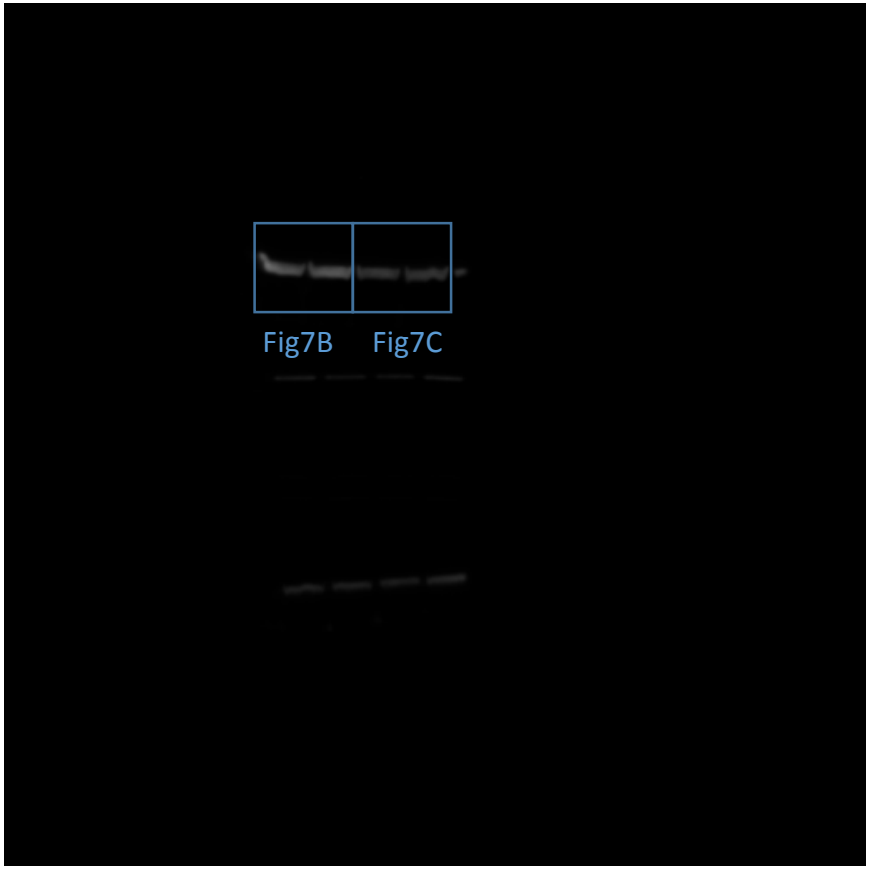

Picture of PVDF membrane

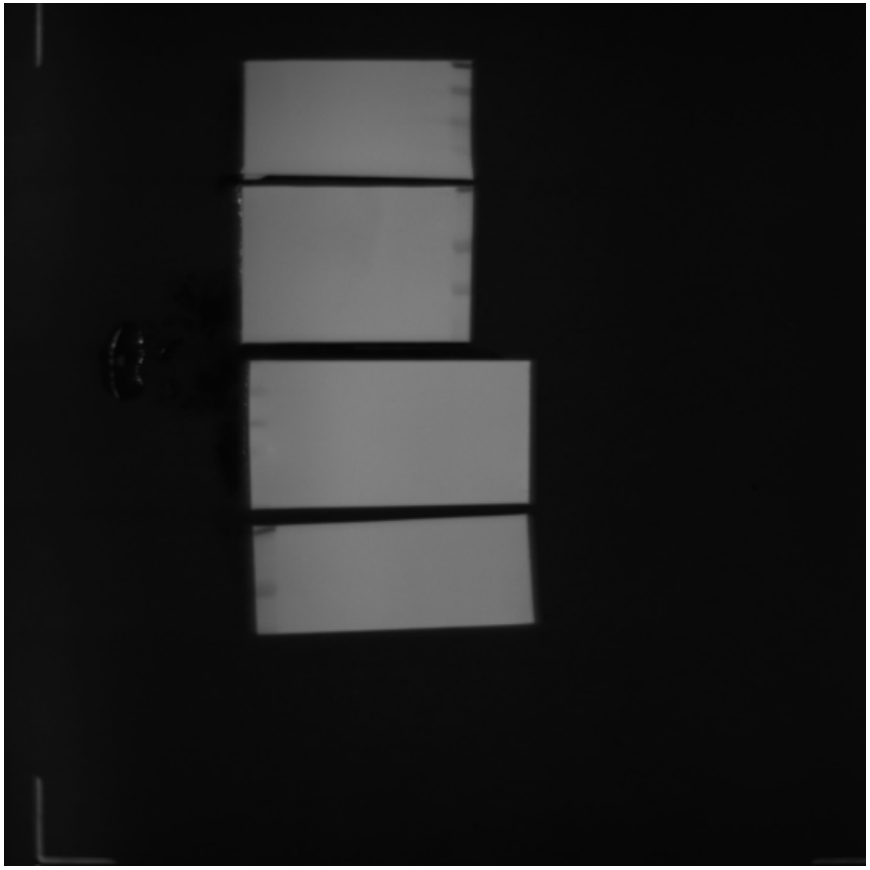

Full images for Figure 7D

Blot for MTP18

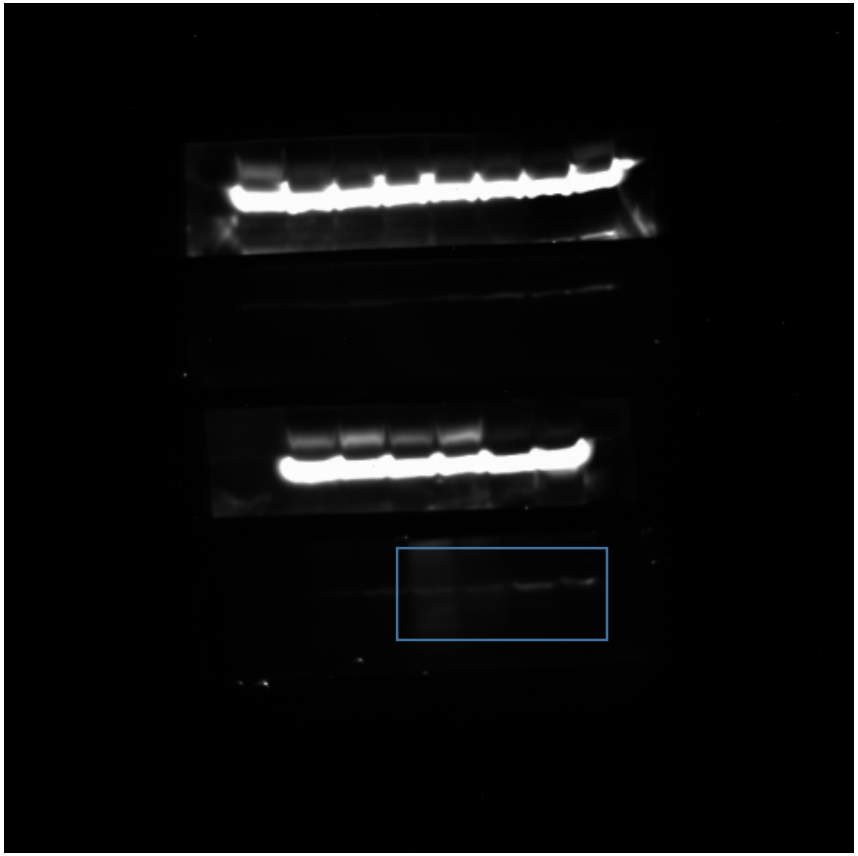

Picture of PVDF membrane

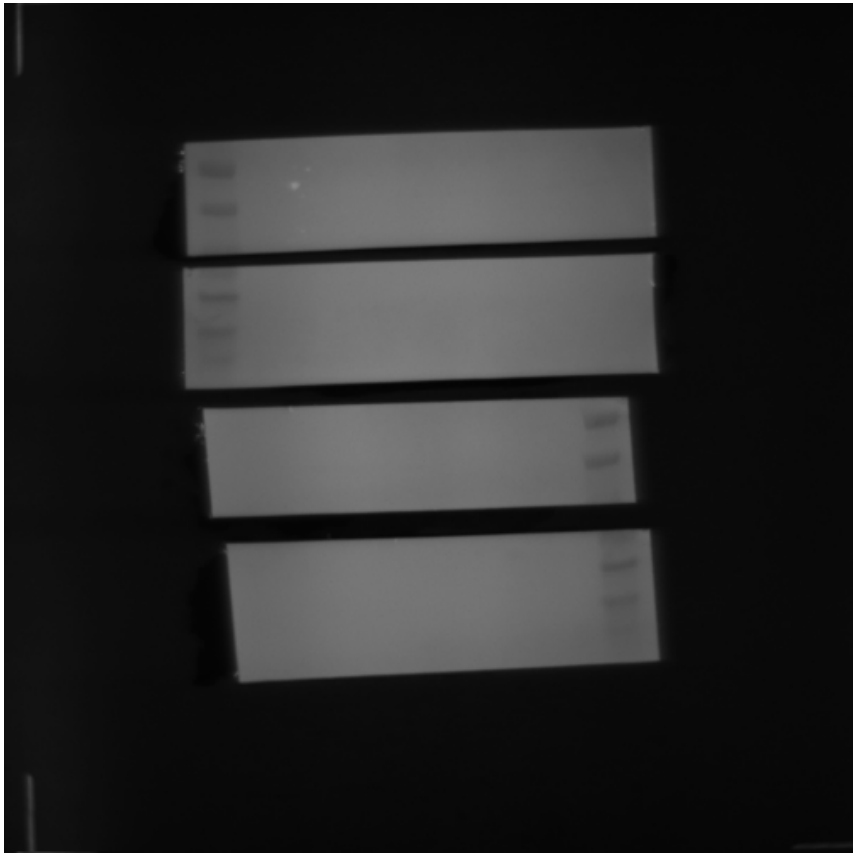

Full images for Figure 7D

Blot for β-actin

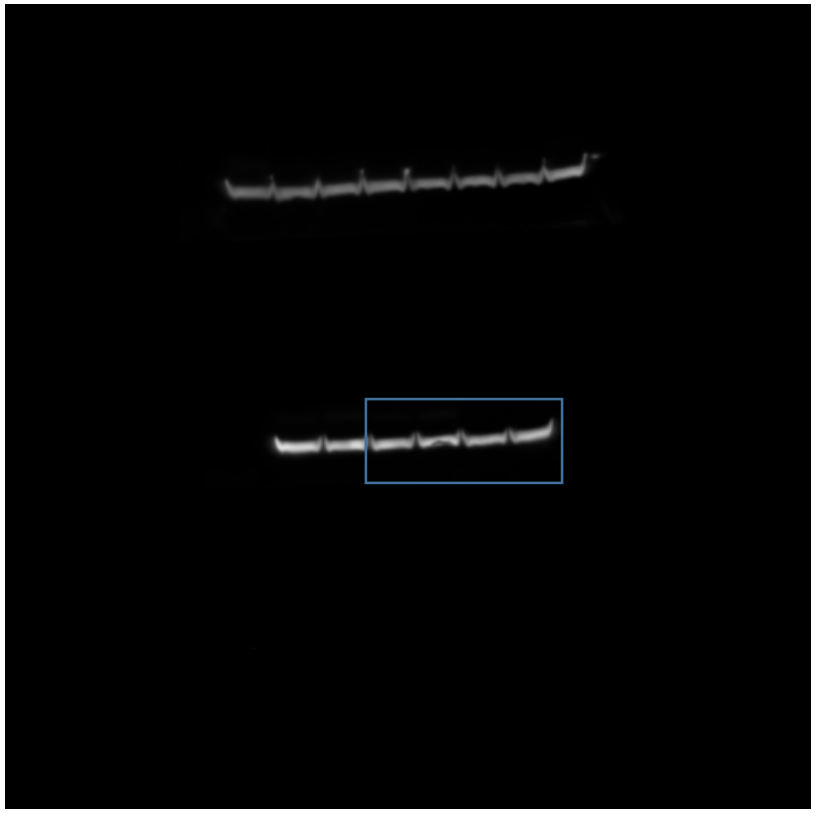

Picture of PVDF membrane

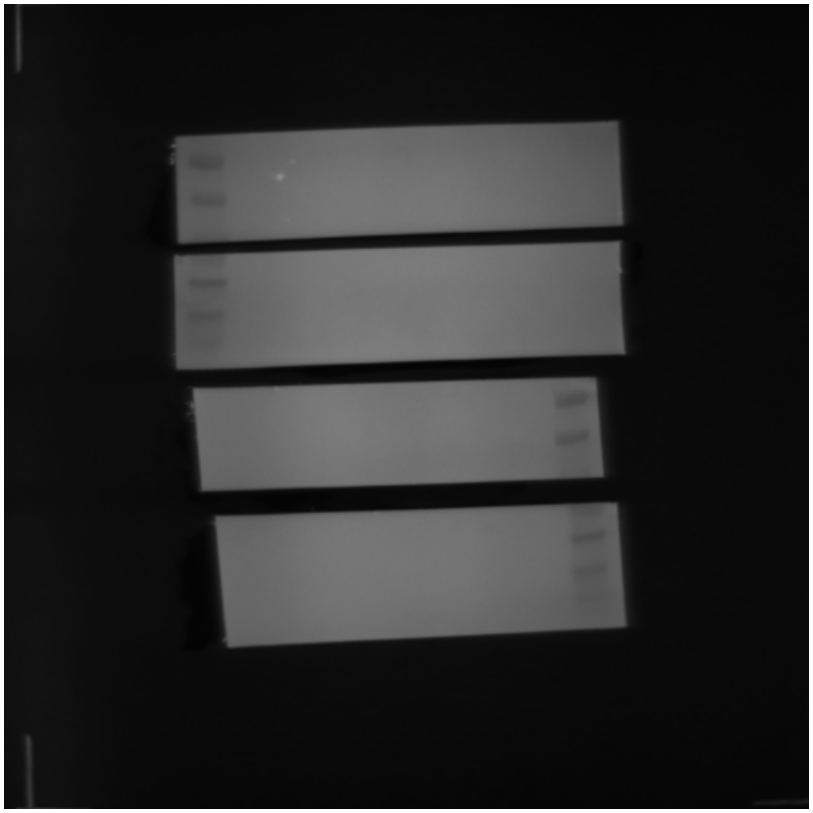

Full images for Figure 7E

Blot for MTP18

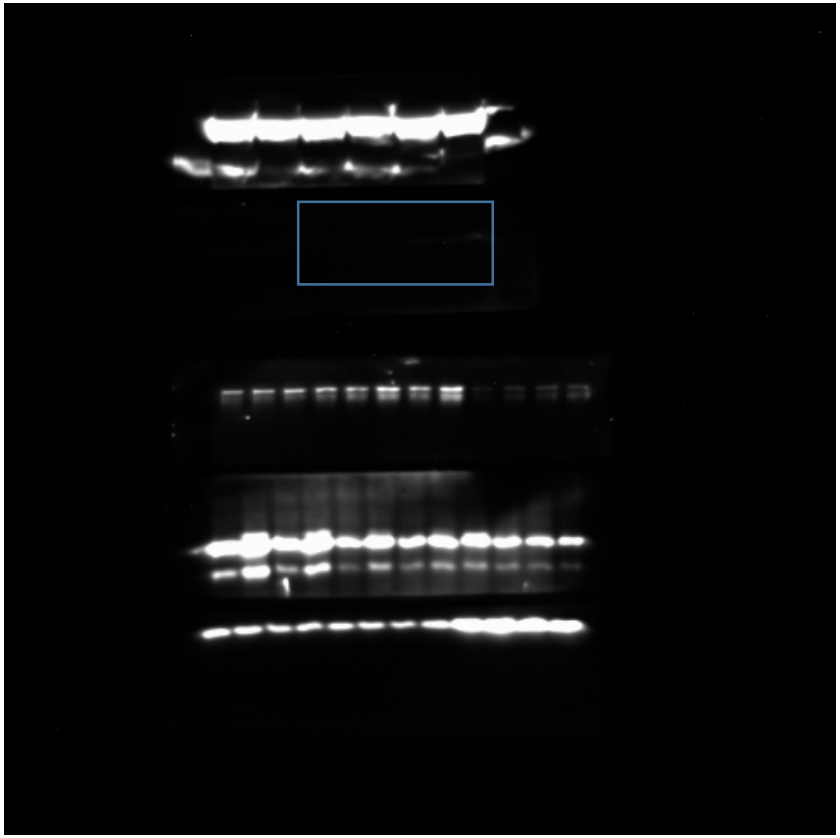

Picture of PVDF membrane

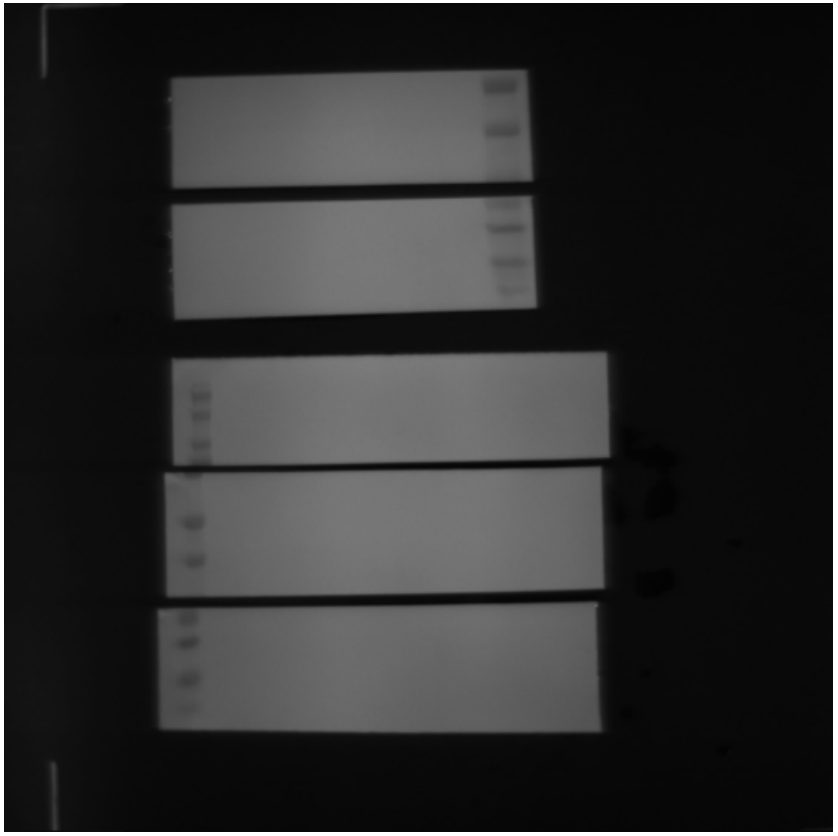

Full images for Figure 7D

Blot for β-actin

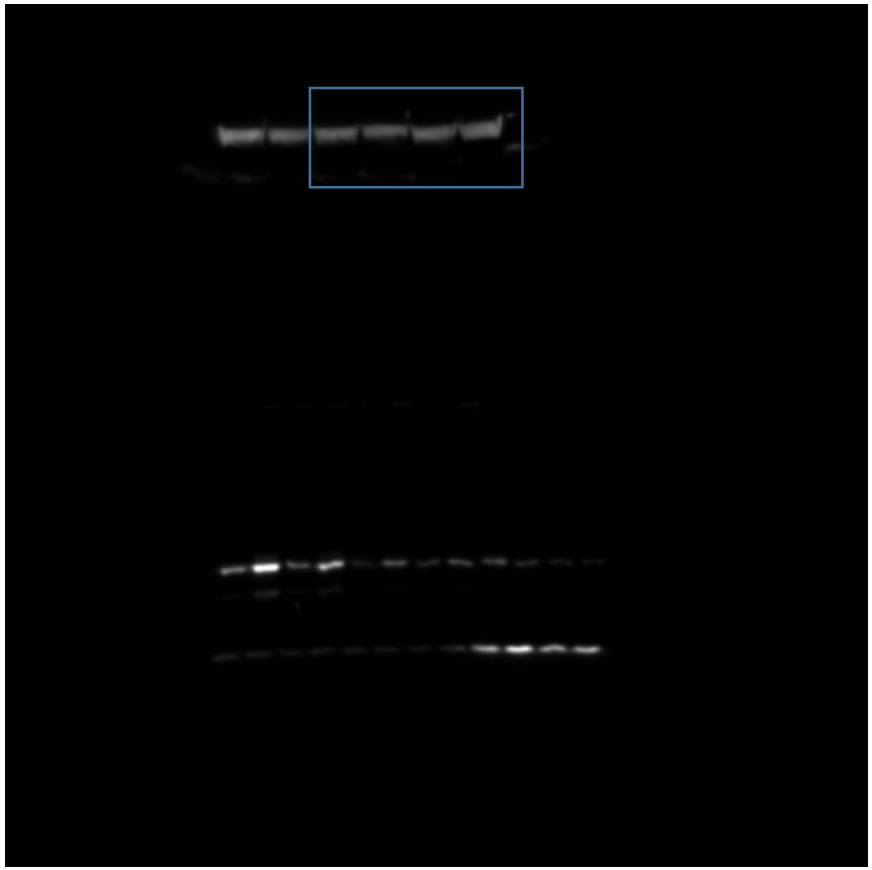

Picture of PVDF membrane

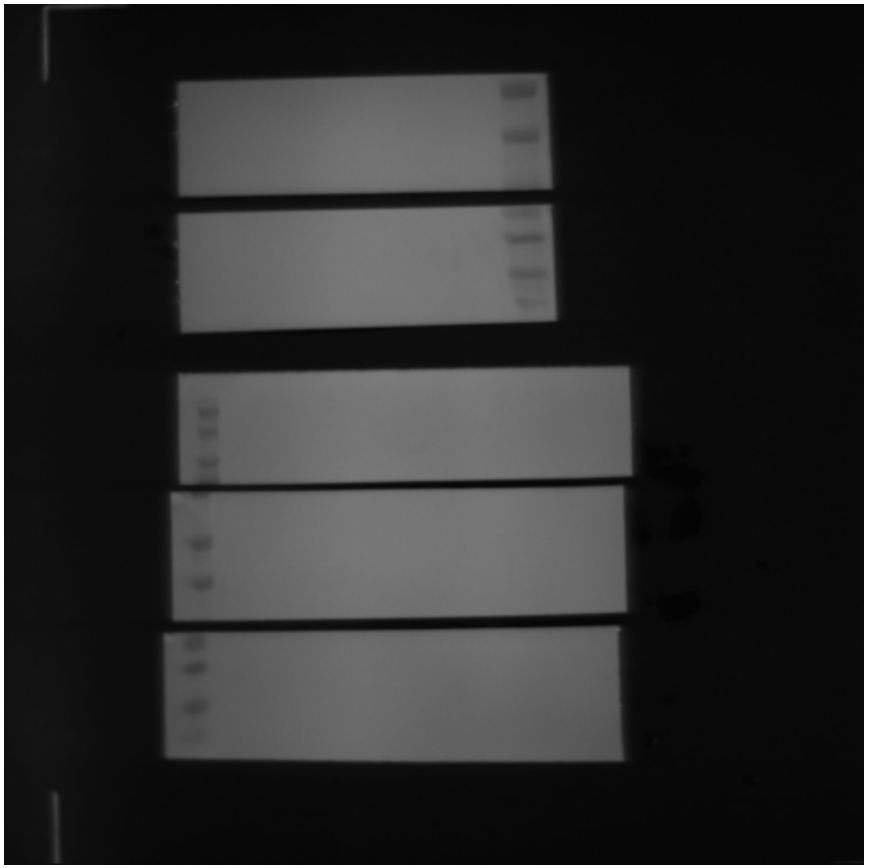

Full images for supplementary Figure 4A

Blot for HIF-1α

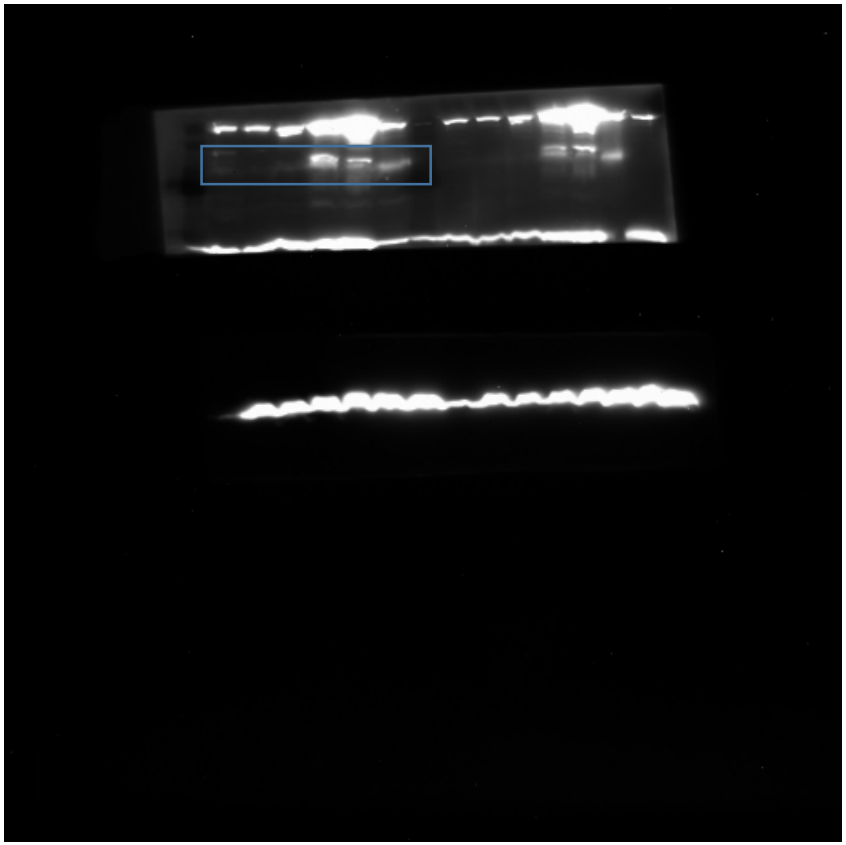

Picture of PVDF membrane

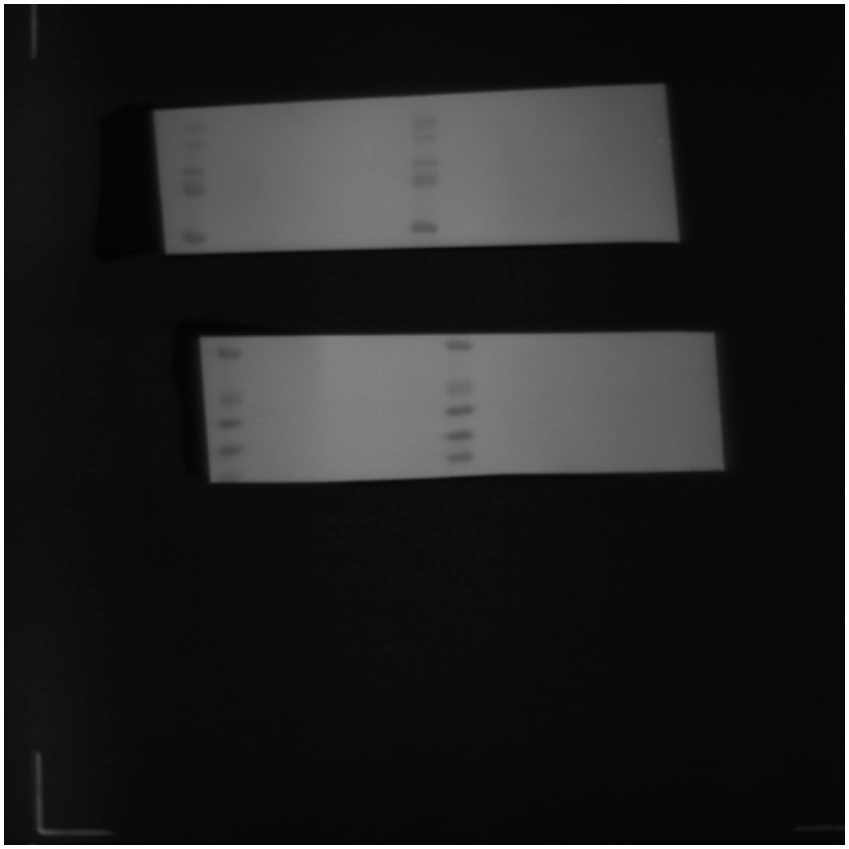

Full images for supplementary Figure 4A

Blot for cyclophilin b

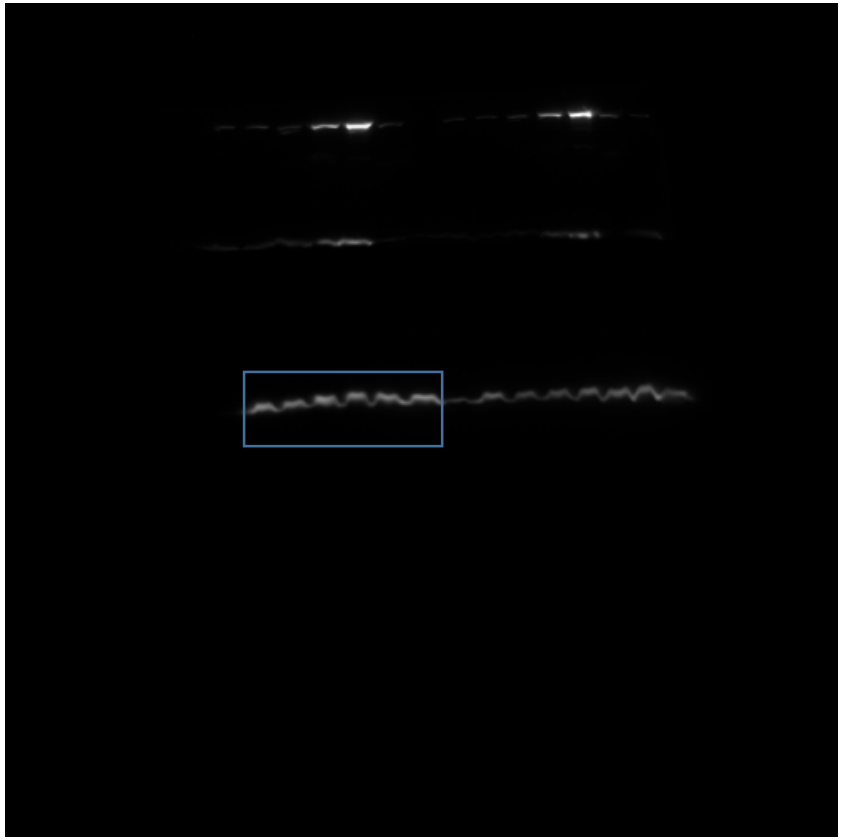

Picture of PVDF membrane

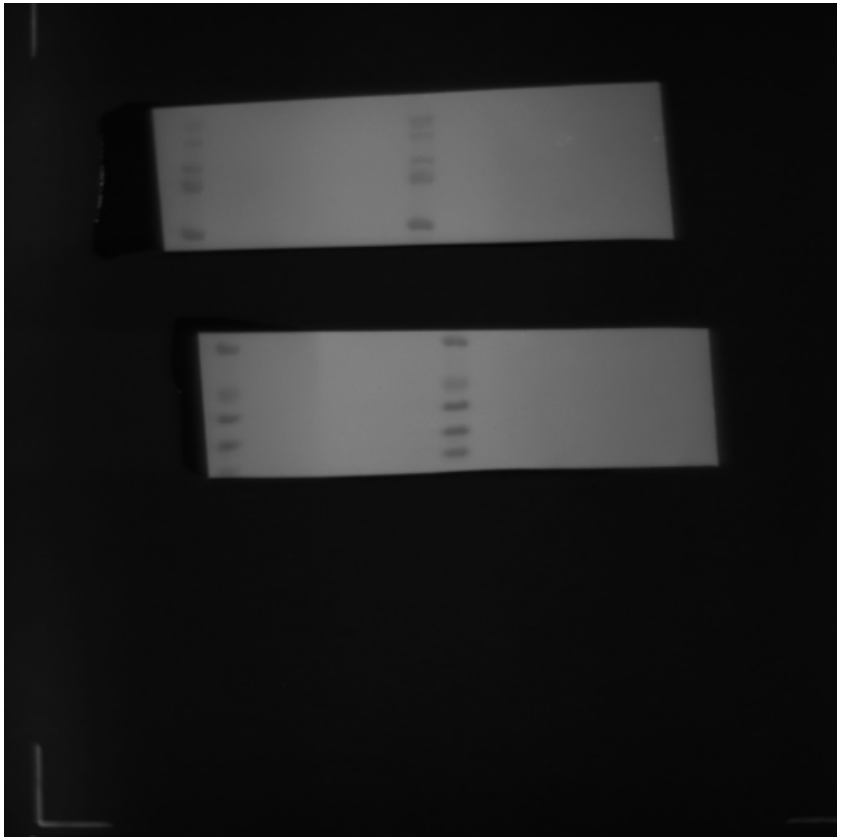

Full images for supplementary Figure 4A

Blot for MTP18

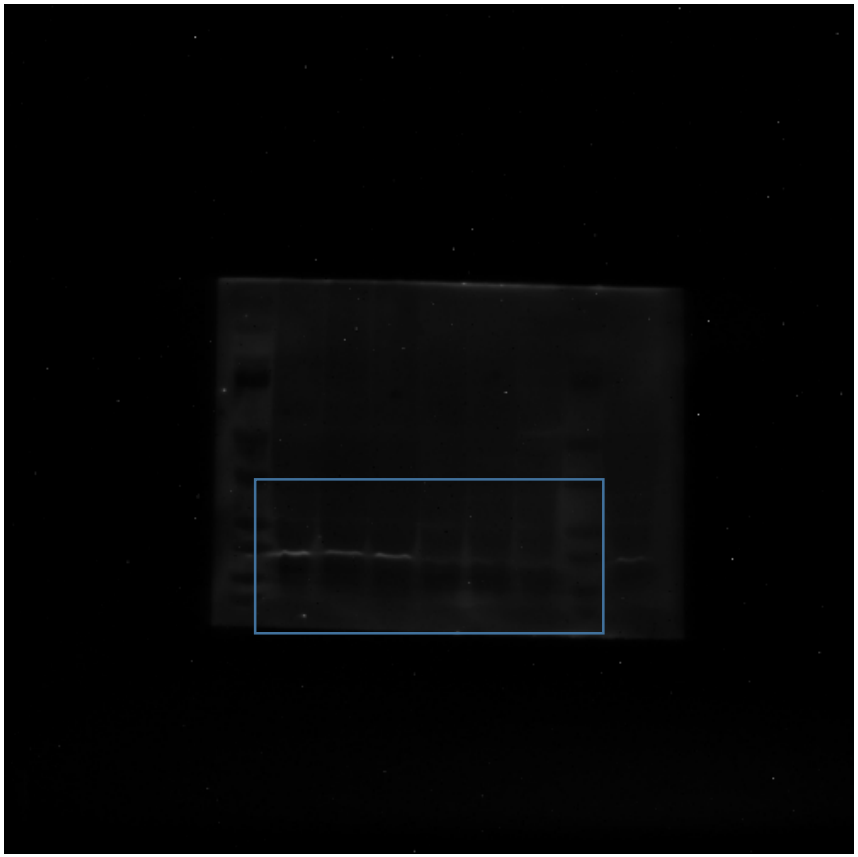

Picture of PVDF membrane

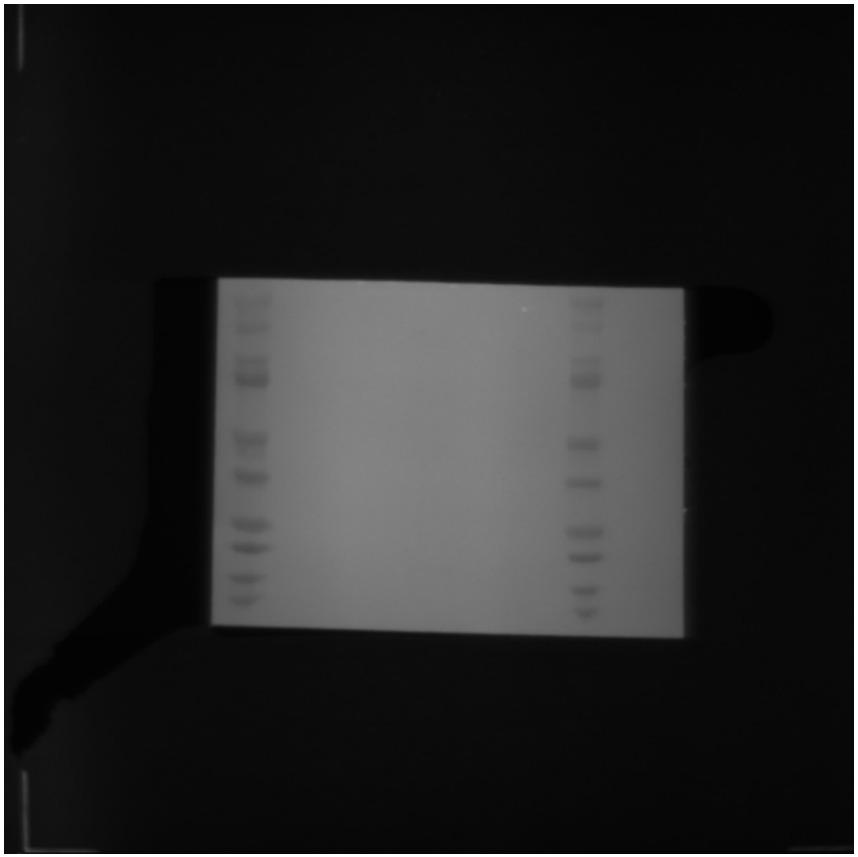

Full images for supplementary Figure 4A

Blot for cyclophilin b (MTP18)

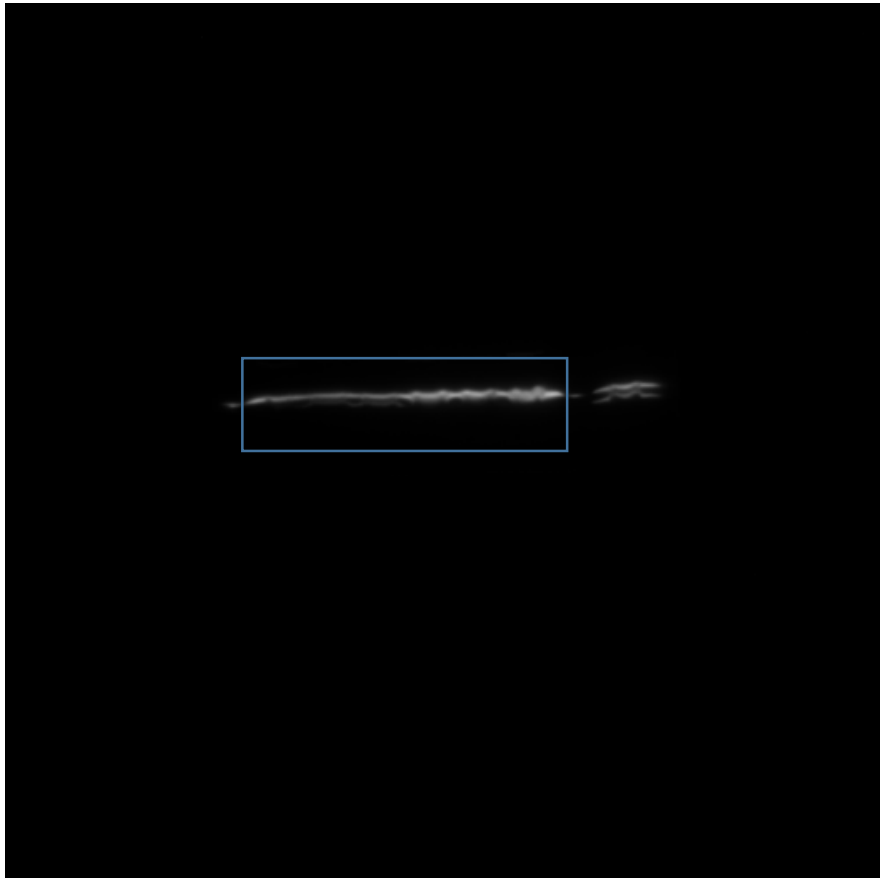

Picture of PVDF membrane

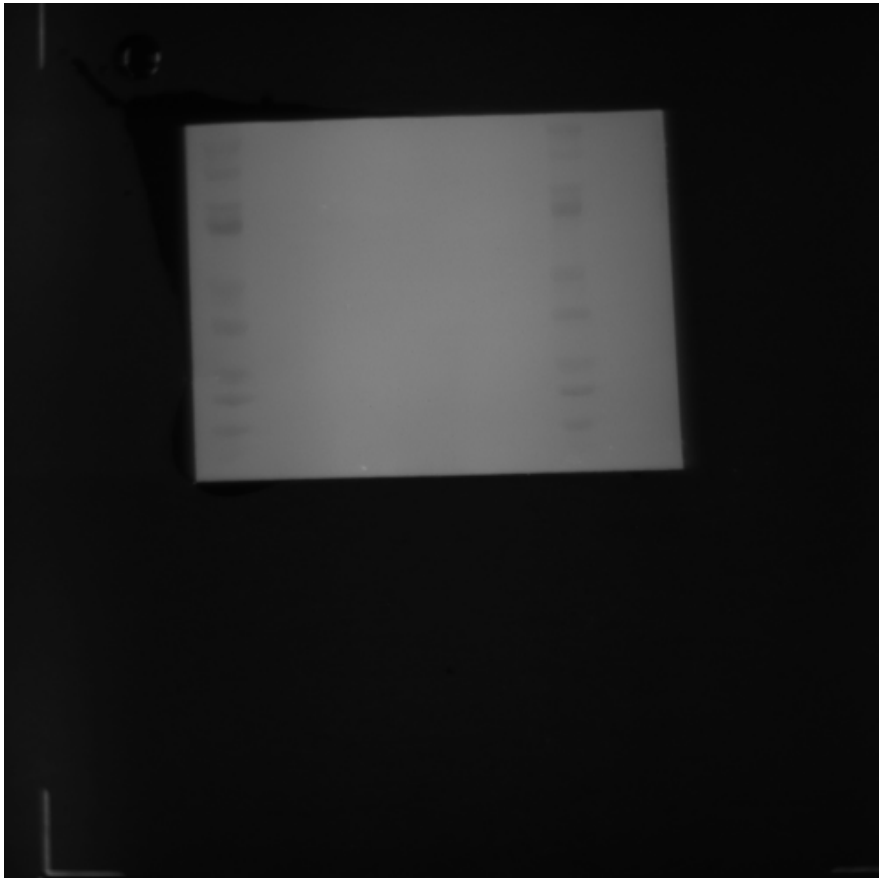

Full images for supplementary Figure 5A

Blots for HIF-1α and cyclophilin b

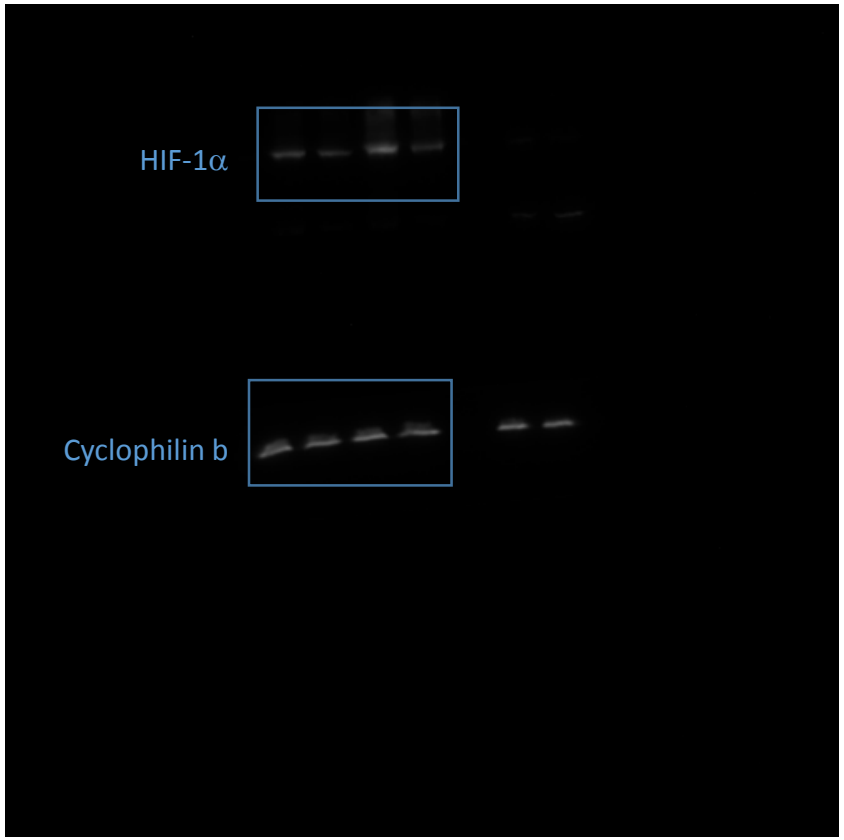

Picture of PVDF membrane